

China Flux 2019 Eddy Covariance Instrumentation

Ivan Bogoev, Larry Jacobsen, Eduard Swiatek
Ben Conrad, Bert Tanner

CAMPBELL SCIENTIFIC



China Flux 2019

Topic:
The fundamental working principals and major field applications of sonic anemometer, CO₂/H₂O/trace gas analyzer, and atmospheric profile system

Contents

- a. How 3D sonic anemometer measures 3D wind
- b. Definition and calculation of sonic temperature
- c. Measurement working models of 3D wind speeds and sonic temperature
- d. Frequency response of sonic anemometer
- e. Optical principals of measuring CO₂, H₂O, and some trace gas species
- f. Spectrum absorption of CO₂, H₂O, and some trace gas species
- g. Beer-Bouguer Law
- h. Measurement working models of gas analyzer
- i. Frequency response of gas analyzer
- j. Applications of sonic anemometer, infrared gas analyzers in OPEC, CPEC and AP systems.
- k. Applications of laser trace gas analyzers in flux measurements.

The beginning in 2002: Changbaishan



Passion, Dedication and Commitment to Flux Measurements

The beginning in 2002: Changbaishan



Passion, Dedication and Commitment to Flux Measurements

The beginning in 2002: Changbaishan



Passion, Dedication and Commitment to Flux Measurements

Acknowledgements for contributions from:

T. Foken, J. Wingard, M. Aubinet, J. Kaimal, J. Finnigan, R. Leuning, T. Horst, G. Burba, A. Grelle, R. Vogt, S. Oncley

The collage includes the following items:

- ATMOSPHERIC BOUNDARY LAYER FLOWS: THEIR STRUCTURE AND MEASUREMENTS** by J. C. Kaimal (Elsevier)
- A Brief Practical Guide to Eddy Covariance Flux Measurements** (Principles and Workflow Examples for Scientific and Industrial Applications)
- Eddy Covariance: A Practical Guide to Measurement and Data Analysis** edited by Marc Aubinet, Timo Vesala, and Dario Papale
- Fine-wire thermometer to correct CO₂ fluxes by open-path analyzers for artificial density fluctuations** (Boundary-Layer Meteorol, DOI: 10.1007/s10546-015-0123-8)
- Evaluation of Probe-Induced Flow Distortion of Campbell CSAT3 Sonic Anemometers by Numerical Simulation** by Sadiq Hsuq¹, Frederik De Roo¹, Thomas Foken², and Matthias Mauder¹ (Boundary-Layer Meteorol, DOI: 10.1007/s10546-015-0010-3)
- Measurements of Flow Distortion within the IRGAS Integrated Sonic Anemometer and CO₂/H₂O Gas Analyzer** (T. W. Horst¹, R. Vogt², S. P. Oncley¹)
- Correction of a Non-orthogonal, Three-Component Sonic Anemometer for Flow Distortion by Transducer Shadowing** (T. W. Horst¹, S. R. Semmer¹, G. Macken)
- The Importance of Water Vapor Measurements and Corrections** (Application Note 018)

What is an eddy?

"Eddies within eddies from near and far..."



Eddy Covariance Tall Tower Installation



Eddy Covariance Measurement Principles

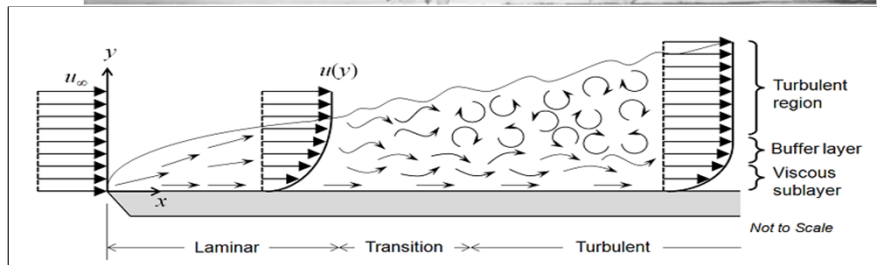
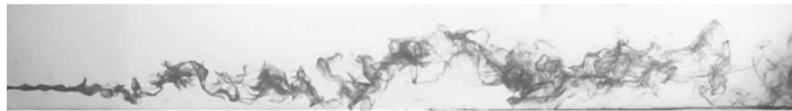
“Vortices swirl around each star,
Eddies within eddies from near and far...”



Vincent van Gogh “Starry Night” 1889

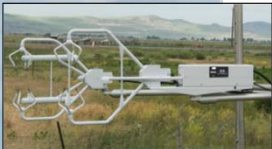
Google Art Project

Mechanism of Turbulence Transfer - Eddies



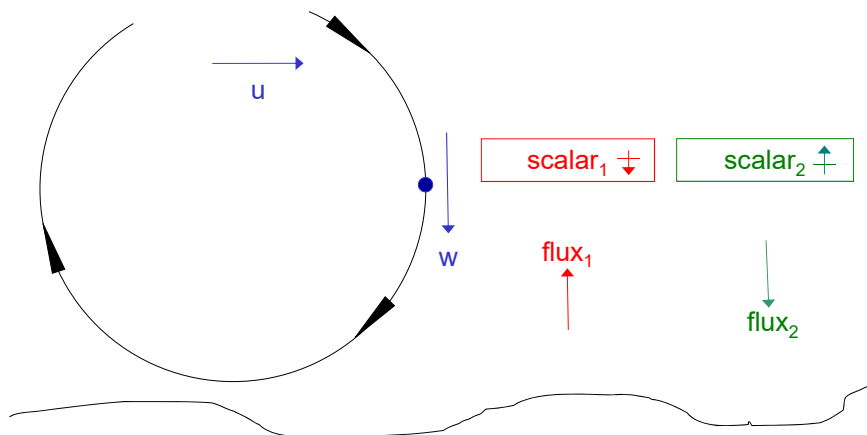
Mechanism of Turbulence Transfer Eddies and Scalars

Turbulent transport measured
by vertical wind and

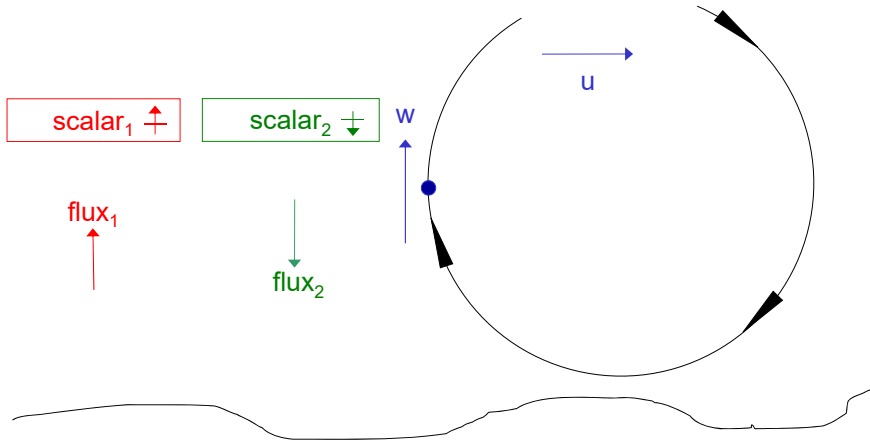


- Temperature: Convection (Sensible Heat)
- Water Vapor: Evaporation (Latent Heat)
- CO₂: Carbon Flux
- CH₄: Methane Flux
- Horizontal Wind: Momentum Flux

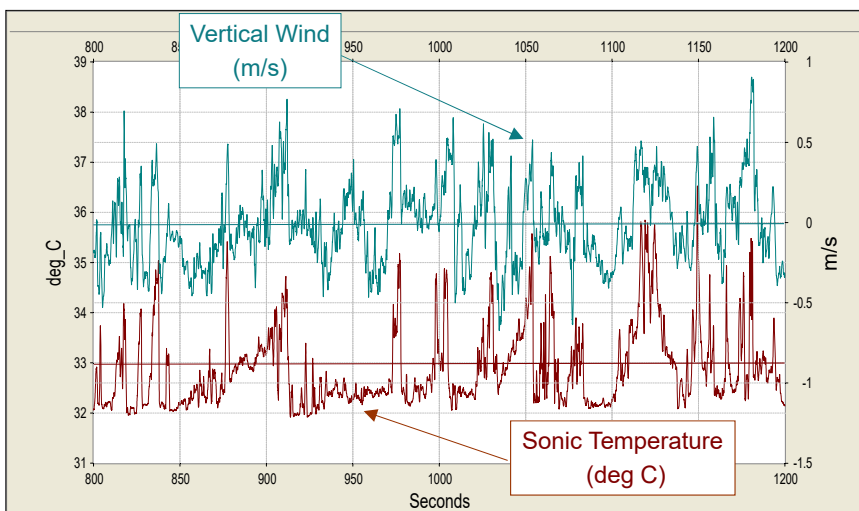
Eddy Covariance Measurement Principles



Eddy Covariance Measurement Principles



Eddy Covariance Time Series



Eddy Covariance Measurement Principles

Reynolds decomposition of time series:

$$\zeta = \bar{\zeta} + \zeta' \quad \bar{\zeta} = \frac{1}{T} \int_t^{t+T} \zeta(t) dt$$



$$I \quad \overline{\zeta'} = 0$$

$$II \quad \overline{\zeta\xi} = \bar{\zeta}\bar{\xi} + \overline{\zeta'\xi'}$$

$$III \quad \overline{\zeta\xi} = \bar{\zeta}\bar{\xi}$$

$$IV \quad \overline{a\zeta} = a\bar{\zeta}$$

$$V \quad \overline{\zeta + \xi} = \bar{\zeta} + \bar{\xi}$$

Reynolds averaging rules:

Eddy Covariance Measurement Principles



Ensemble Averaging: averaging over many realizations under identical conditions

Ergodic Hypothesis: time averages are equivalent to ensemble averages when the fluctuations are **statistically stationary** during the averaging time

Eddy Covariance Measurement Principles

Eddy flux:
$$F \approx \overline{\rho_a w' s'}$$

where: ρ_a is the dry air density, w is the vertical wind and s is the scalar (mixing ratio, temperature, etc.) overbar denotes average and prime denotes fluctuations

Assumptions: no divergence/convergence, no storage or accumulation of mass, average fluctuations are zero

Eddy Covariance Measurement Principles

Scalar definition of intensity of a constituent:

(A) in terms of molar density (mole m⁻³)

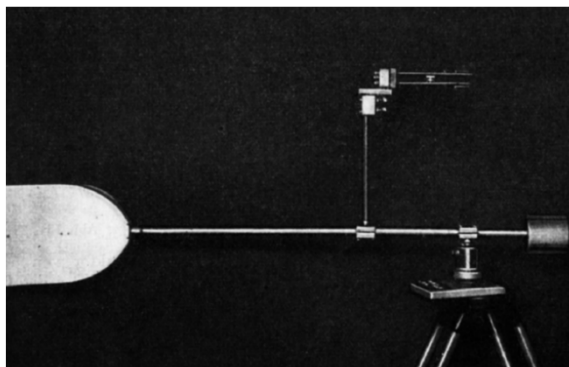
or mass density (kg m⁻³)

(B) in terms of mole fraction (mole mole⁻¹) constituents partial pressure to the total pressure

or mass mixing ratio (kg kg⁻¹) ratio of the mass of constituent to the mass of dry air

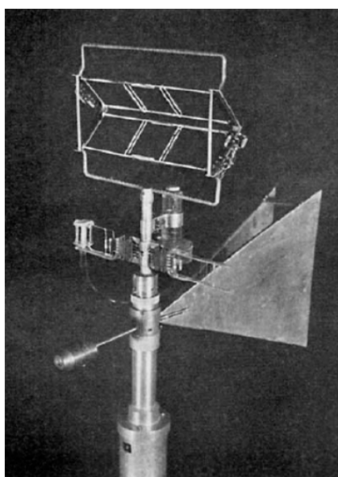
Only (B) are conserved quantities in the presence of changes in temperature, pressure and water vapor content

Early Instruments for Atmospheric Turbulence and Wind Measurements



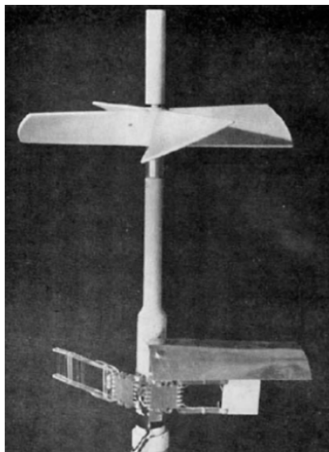
Wind vane with two perpendicular hot wire sensors for measuring friction velocity (Obukhov, 1951)

Early Instruments for Eddy Covariance Measurements



Evapotron
Hot wire anemometer and
psychrometer
Dyer (1965)

Early Instruments for Eddy Covariance Measurements

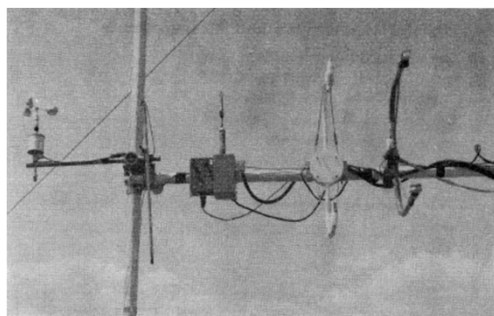


Fluxatron

Propeller anemometer with
fine wire thermometer

Dyer (1967)

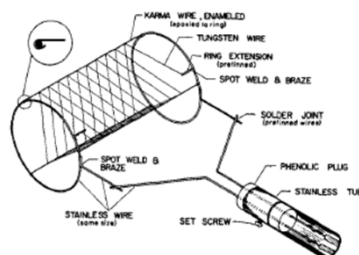
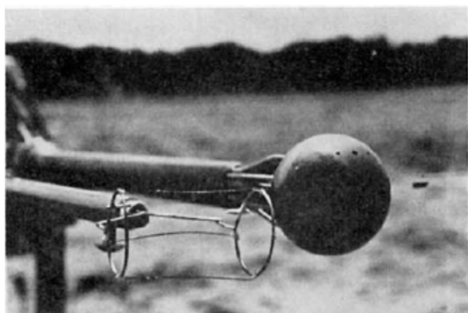
Early Sonic anemometers



Businger (1969) University of Washington

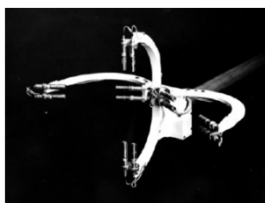
Mitsuta & Hanafusa (1969) Kyoto University

Early Instruments for Eddy Covariance Measurements

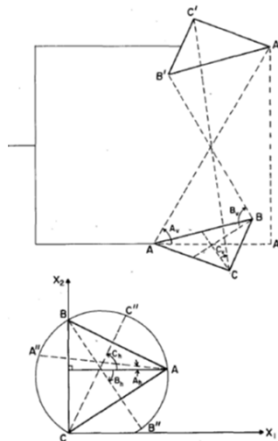
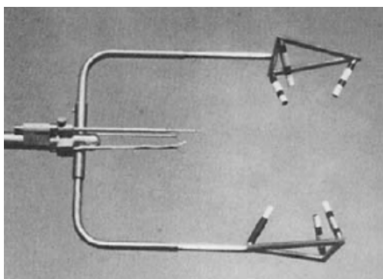


Fine wire PRT and spherical pressure probe for sensible heat flux measurements (Wesely 1970)

Early Sonic anemometers – orthogonal geometry



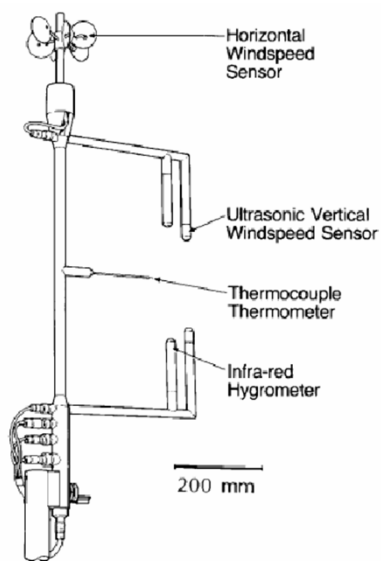
History of the CSAT3 Sonic Anemometer



University of Washington
Non-orthogonal design

U.W. Sonic Anemometer (Zhang, Wyngaard, Businger and Oncley 1986)
Designed to reduce transducer shadowing for the horizontal wind components and increase the range of acceptable wind directions

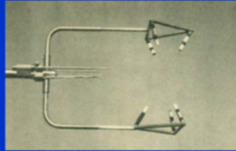
Early Eddy-covariance System Designs



Hydra II

History of the CSAT3 Sonic Anemometer

The Optimal Sonic Anemometer Type




Zhang, S. F., Wyngaard, J. C., Businger, J. A., and Oncley, S. P.: Response characteristics of the U.W. sonic anemometer, *J. Atm. Oceanic Techn.*, 2, 548-558, 1986.

(Reprinted from BULLETIN OF THE AMERICAN METEOROLOGICAL SOCIETY, Vol. 76, No. 7, July 1995) Printed in U. S. A.

Workshop on Instrumental and Methodical Problems of Land Surface Flux Measurements
Thomas Foken* and Steven Oncley*

One year after an international workshop held in Grenoble in 1994, Campbell Sci. Inc. produced CSAT3

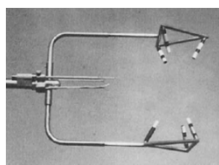


In memoriam
Dr. h.c. Bert Tanner

Slide by T. Foken

21st Symposium on Boundary Layers and Turbulence
9-13 June 2014, Leeds, United Kingdom

Transformation Matrices

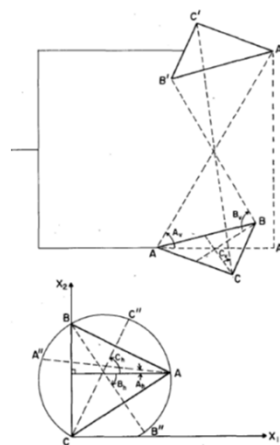


$$S_i = \sum_j a_{ij} U_j, \quad i, j = 1, 2, 3$$

$$a_{ij} = \begin{pmatrix} -\cos A_h \cos A_v & \sin A_h \cos A_v & \sin A_v \\ \cos B_h \cos B_v & -\sin B_h \cos B_v & \sin B_v \\ \cos C_h \cos C_v & \sin C_h \cos C_v & \sin C_v \end{pmatrix}$$

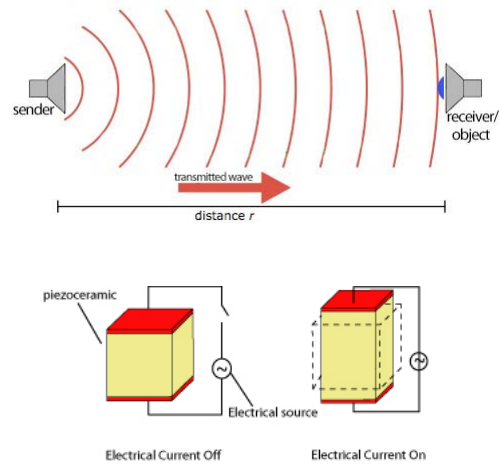
$$U_i = \sum_j b_{ij} S_j, \quad i, j = 1, 2, 3$$

$$b_{ij} = (a_{ij})^{-1}$$

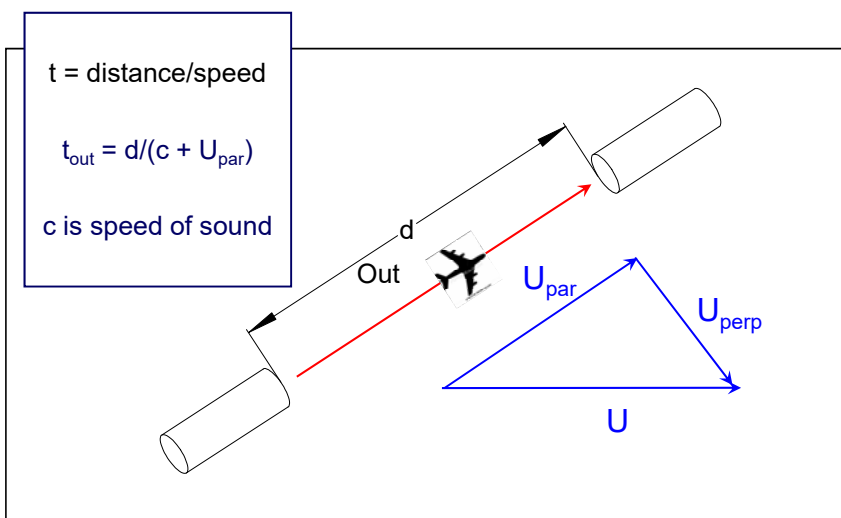


Conversion from orthogonal to non-orthogonal coordinates

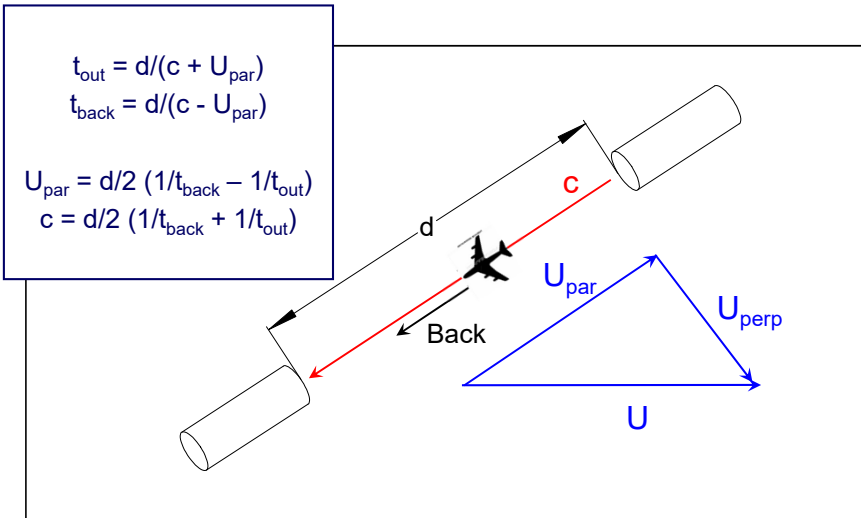
Sonic Anemometer Measurement Principles



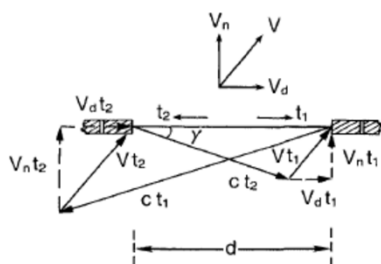
Sonic Anemometer Measurement Principles



Sonic Anemometer Measurement Principles



Speed of Sound Measurement and Cross-Wind Correction



$$V_d = \frac{d}{2} \left(\frac{1}{t_1} - \frac{1}{t_2} \right) \quad \frac{1}{t_1} + \frac{1}{t_2} = \frac{2}{d} c \cos \gamma$$

$$= \frac{2}{d} (c^2 - V_n^2)^{1/2}$$

$$c^2 = \frac{d^2}{4} \left(\frac{1}{t_1} + \frac{1}{t_2} \right)^2 + V_n^2$$

$$c^2 = 403 T(1 + 0.32e/p), \quad e=0$$

dry air

$$T_v = \frac{d^2}{1612} \left(\frac{1}{t_1} + \frac{1}{t_2} \right)^2 + \frac{1}{403} V_n^2$$

Implemented in the firmware of the CSAT3

$$c = \sqrt{\frac{1.4RT}{M}}$$

Acoustic Virtual Temperature is determined using Gas constant and Specific heat for **dry air**

Accuracy of Acoustic Temperature Measurement



$$T_v = \frac{d^2}{1612} \left(\frac{1}{t_1} + \frac{1}{t_2} \right)^2 + \frac{1}{403} V_n^2$$

The distance (**d**) between the transducer faces needs to be measured accurately

A deviation of 0.1 mm (a thickness of a sheet of paper) will result in a temperature error of about 0.3K

Research grade anemometers can resolve 0.002K

Transducer delays need to be calibrated over the entire operating temperature range

Acoustic Virtual Temperature Measurement

$$c = \sqrt{\gamma_d R_d T \cdot \left(1 + \left(\frac{\gamma_v}{\gamma_d} - \frac{M_v}{M_d} \right) \cdot \frac{e}{p - \left(1 - \frac{M_v}{M_d} \right) \cdot e} \right)}$$

Speed of sound in **humid air**

$$T_{av} = T \cdot \left(1 + \left(\frac{\gamma_v}{\gamma_d} - \frac{M_v}{M_d} \right) \cdot \frac{e}{p - \left(1 - \frac{M_v}{M_d} \right) \cdot e} \right)$$

Acoustic Temperature depends on the humidity of the air

Acoustic Temperature > Air Temperature

Acoustic Temperature approximates virtual temperature

Acoustic Virtual Temperature Measurement

$$T_{av} = T \cdot \left(1 + \left(\frac{\gamma_v}{\gamma_d} - \frac{M_v}{M_d} \right) \cdot \frac{e}{p - \left(1 - \frac{M_v}{M_d} \right) \cdot e} \right)$$

The perfect instrument idea: all measurements are in the same volume
 IRGASON can provide true air temperature because of the synchronized and co-located water vapor measurement

$$T'_s = T' + 0.51q'\bar{T}$$

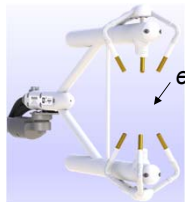
Standalone sonic anemometer are not able to measure true air temperature
 The sonic virtual temperature spectrum is contaminated by water vapor fluctuations scaled by absolute temperature
 q – specific humidity [kg kg⁻¹] (moist air)

$$\overline{w'T'_s} = \overline{w'T'} + 0.51 \bar{T} \overline{w'q'}$$

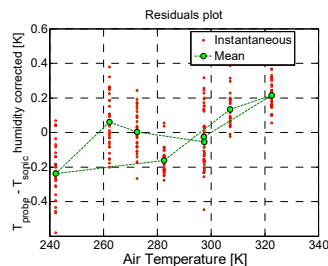
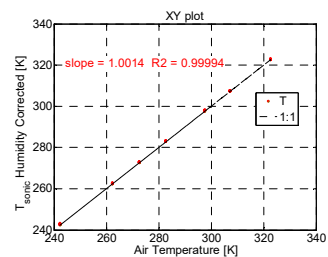
Sonic heat flux need a latent heat flux correction

Fast-response Acoustically derived Air Temperature Measurement

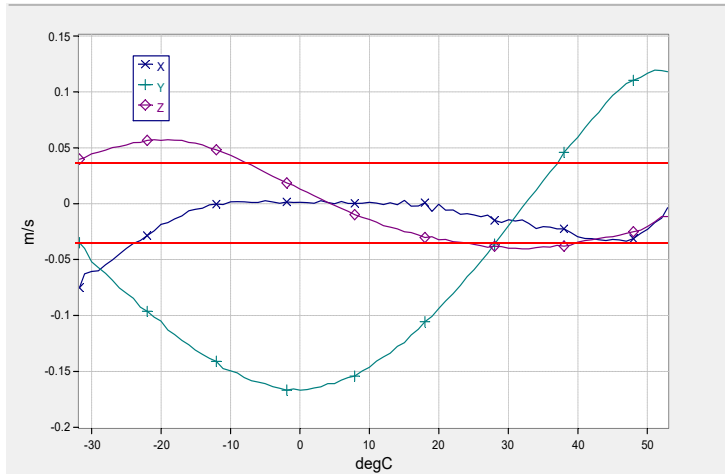
$$T_{av} = T \cdot \left(1 + \left(\frac{\gamma_v}{\gamma_d} - \frac{M_v}{M_d} \right) \cdot \frac{e}{p - \left(1 - \frac{M_v}{M_d} \right) \cdot e} \right)$$



IRGASON can provide true air temperature because of the synchronized and co-located water vapor measurement



Sonic Anemometer Calibration



Wind Offset and Distance Calibration: Temperature range -30 to +50 deg. C
 Piezoelectric transducers are resonant devices and have certain delay when excited. These delays are accounted during calibration in a zero-
 Maximum Offset Error <math>< \pm 8.0 \text{ cm s}^{-1}</math> (u_x, u_y), <math>< \pm 4.0 \text{ cm s}^{-1}</math> (u_z)

Sonic Anemometer Calibration

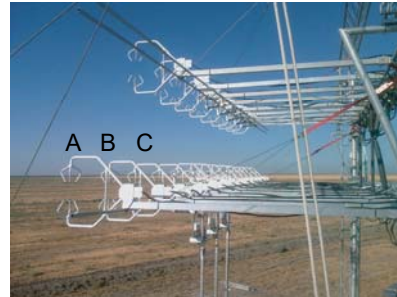
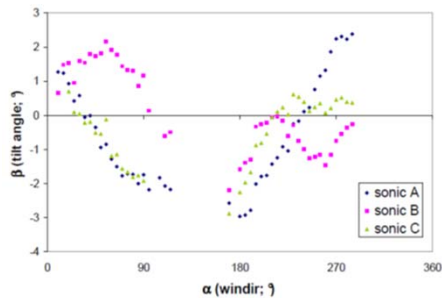


Zero-wind box with dry air

Wind Offset and Distance Calibration: Temperature range -30 to +50 deg. C

Maximum Offset Error <math>< \pm 8.0 \text{ cm s}^{-1}</math> (u_x, u_y), <math>< \pm 4.0 \text{ cm s}^{-1}</math> (u_z)

Sonic Anemometer Coordinate Rotations



What is the frame of reference?

It is difficult (or impossible) to align the sonic coordinate system with an objective frame relative to the local flow field (not gravity)

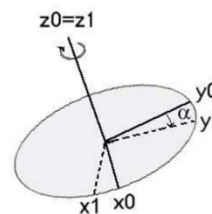
If the sonic is not oriented with the stream flow there will be **cross-contamination between u' and w'**

z-axis should be perpendicular to the mean streamlines surface (and parallel to the scalar concentration gradient)

Sonic Anemometer Coordinate Rotations

Rotation around z-axis (yaw angle) aligns to mean (30 min) wind direction

$$\begin{pmatrix} \bar{u}_1 \\ \bar{v}_1 \\ \bar{w}_1 \end{pmatrix} = \underbrace{\begin{pmatrix} \cos \alpha & \sin \alpha & 0 \\ -\sin \alpha & \cos \alpha & 0 \\ 0 & 0 & 1 \end{pmatrix}}_{R_{01}} \begin{pmatrix} \bar{u}_0 \\ \bar{v}_0 \\ \bar{w}_0 \end{pmatrix}$$

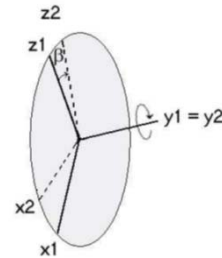


$$\alpha = \tan^{-1} \left(\frac{\bar{v}_0}{\bar{u}_0} \right)$$

Sonic Anemometer Coordinate Rotations

Rotation around new y-axis (pitch angle) nullifies mean vertical wind

$$\begin{pmatrix} \bar{u}_2 \\ \bar{v}_2 \\ \bar{w}_2 \end{pmatrix} = \underbrace{\begin{pmatrix} \cos \beta & 0 & \sin \beta \\ 0 & 1 & 0 \\ -\sin \beta & 0 & \cos \beta \end{pmatrix}}_{R_{12}} \begin{pmatrix} \bar{u}_1 \\ \bar{v}_1 \\ \bar{w}_1 \end{pmatrix}$$



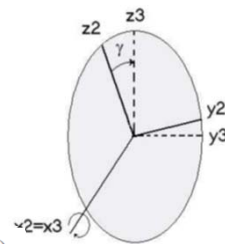
$$\beta = \tan^{-1} \left(\frac{\bar{w}_1}{\bar{u}_1} \right)$$

Sonic Anemometer Coordinate Rotations

Rotation around new x-axis (roll angle) nullifies w'v' **NOT RECOMMENDED ANYMORE**

Finnigan, J. J.: 2004, 'A re-evaluation of long-term flux measurement techniques Part II: Coordinates systems', *Boundary-Layer Meteorology*, 113, 1-41

$$\begin{pmatrix} \bar{u}_3 \\ \bar{v}_3 \\ \bar{w}_3 \end{pmatrix} = \underbrace{\begin{pmatrix} 1 & 0 & 0 \\ 0 & \cos \gamma & \sin \gamma \\ 0 & -\sin \gamma & \cos \gamma \end{pmatrix}}_{R_{23}} \begin{pmatrix} \bar{u}_2 \\ \bar{v}_2 \\ \bar{w}_2 \end{pmatrix}$$



$$\gamma = \frac{1}{2} \tan^{-1} \left(2 \frac{\overline{v_2' w_2'}}{(\overline{v_2'^2} - \overline{w_2'^2})} \right)$$

Rotations are applied for each averaging period

Sonic Anemometer Coordinate Rotations

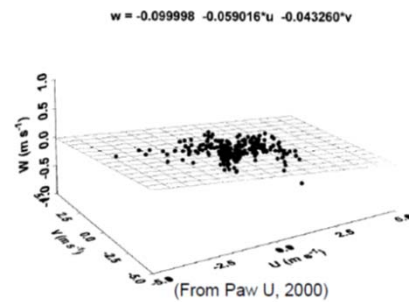
Long-term Planar Fit

Aligns the z-axis perpendicular to the long-term (weeks) mean streamline plane (**long data set** when the position of the sonic does not change).

Planar regression on wind components in the sonic coordinate system:

$$\bar{w}_0 = b_0 + b_1 \bar{u}_0 + b_2 \bar{v}_0$$

b_0 accounts for instrument offset
 b_1 and b_2 define the orientation of the long-term streamline plane



Sonic Anemometer Coordinate Rotations

Long-term Planar Fit

R1: around z-axis, with α nullifies mean crosswind

R2: around y-axis with β_{PF}

R3: around x-axis with γ_{PF}

$$\alpha = \tan^{-1} \left(\frac{\bar{v}_0}{\bar{u}_0} \right)$$

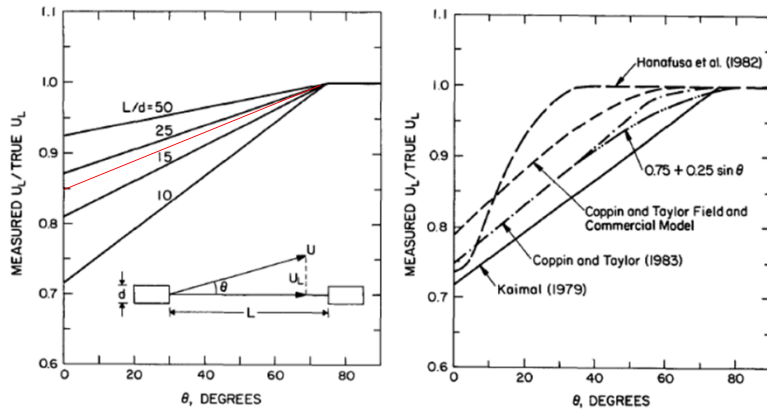
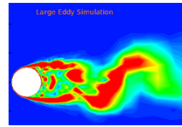
$$\bar{w}_0 = b_0 + b_1 \bar{u}_0 + b_2 \bar{v}_0$$

$$\beta_{PF} = \tan^{-1}(-b_1)$$

$$\gamma_{PF} = \tan^{-1}(b_2)$$

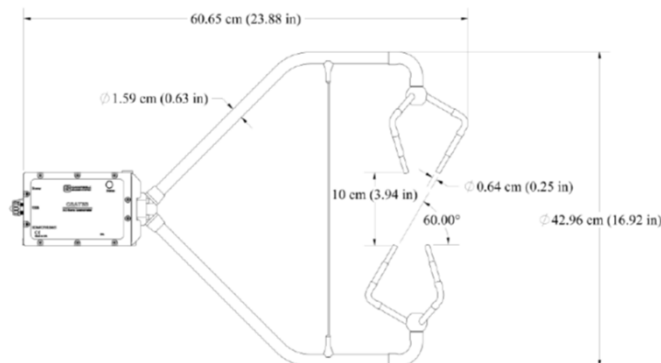
Mean long term vertical velocity = 0 ,
 but not short term (30 min)

Transducer-Shadow Effects



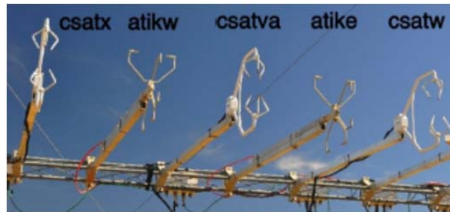
Difficult to characterize in turbulent conditions because there is no standard

Transducer-Shadow Effects



L/d ratio 17.2
 Acoustic paths oriented at a zenith angle of 30 degrees while other designs the angle is 45 degrees with L/d ratio of 9

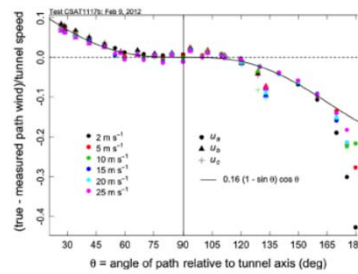
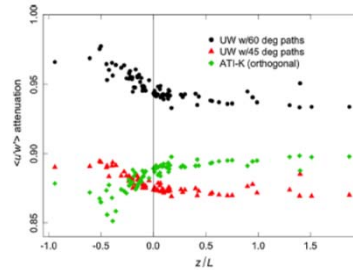
Experiment to Evaluate Transducer-Shadow Effects. What is the optimal geometry?



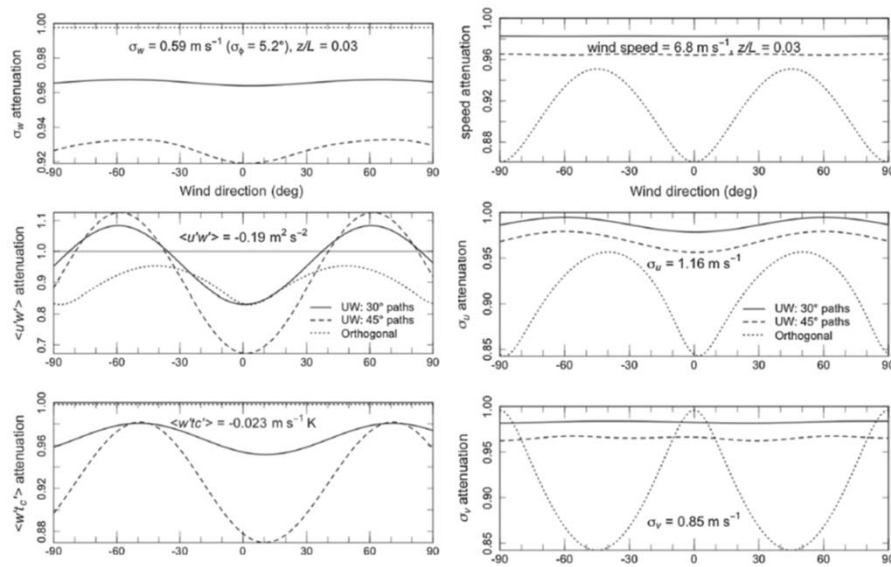
$$\hat{u}_a = u_a (0.84 + 0.16 \sin \theta_a)$$

After Wyngaard and Zhang (1985)

Correction derived in a wind tunnel under laminar flow conditions, but there is **no standard for turbulence**. All we can do is compare instruments or CFD

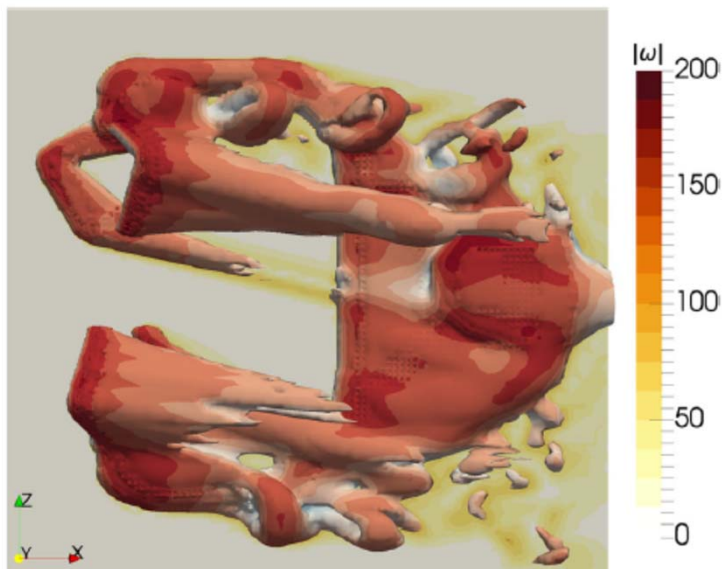


Transducer-Shadow Effects After Horst (2015)

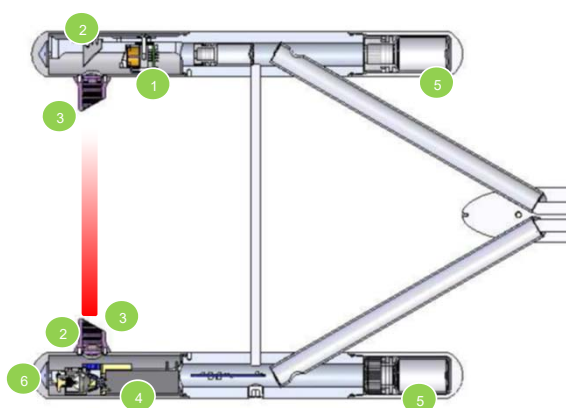


Transducer-Shadow Effects

After Huq et al. (2017)

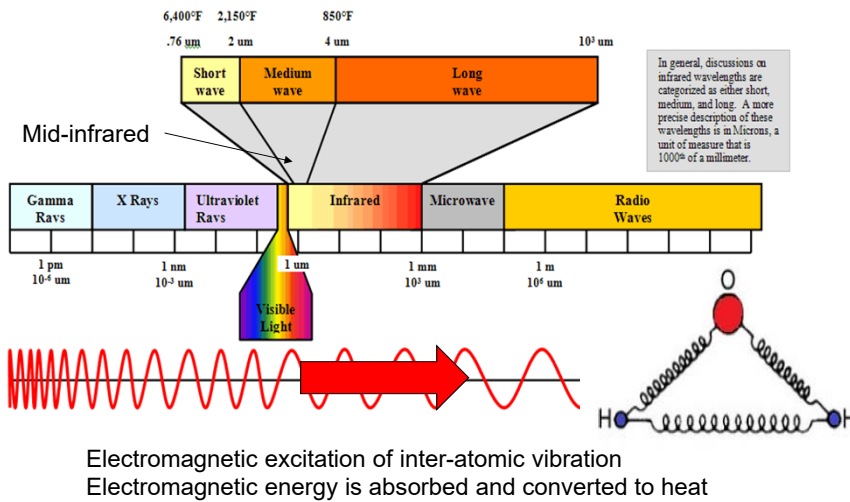


Gas Analyzer Measurement Principles

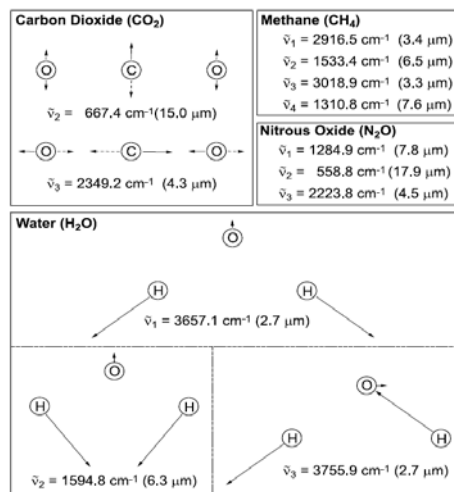


- | | |
|-----------------------------------|--|
| 1 Temperature controlled detector | 4 Brushless chopper motor |
| 2 Precision optical components | 5 CO ₂ and H ₂ O scrubbers |
| 3 Scratch resistant windows | 6 Infrared source |

CO₂ and H₂O Infrared Gas Analyzer Measurement Principles



Gas Analyzer Measurement Principles

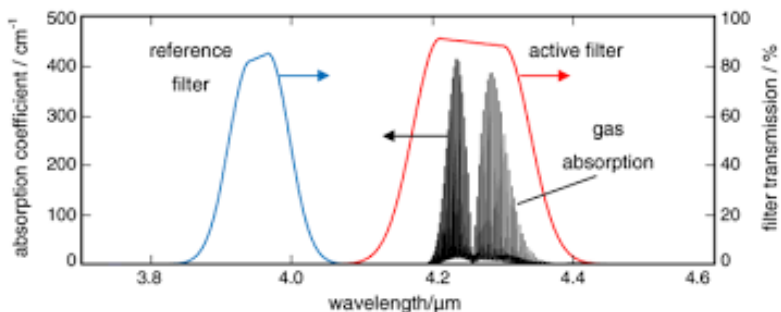


Different Vibration modes of some GHG with strong absorption coefficients

CO₂: asymmetrical stretching at 4.3 μm

H₂O: asymmetrical stretching at 2.7 μm

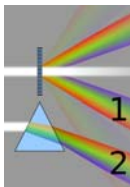
CO₂ Absorption Bands in the Infrared



Dispersive

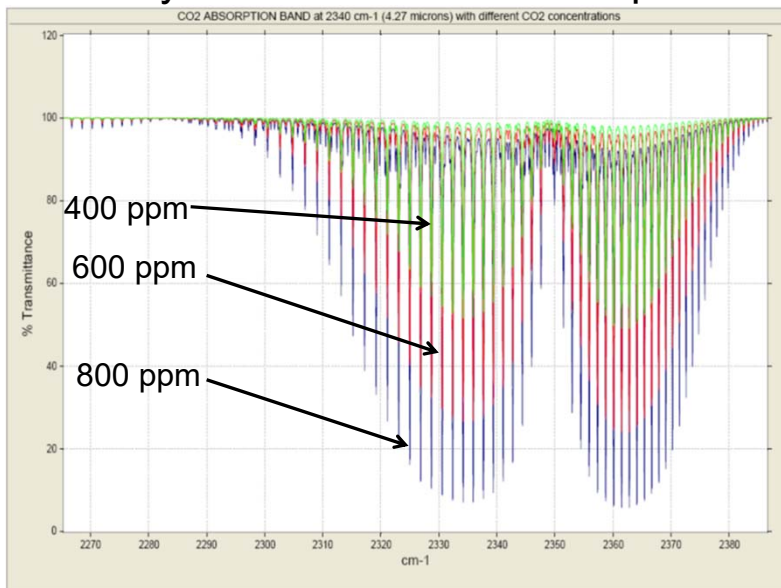
Non-dispersive

4 Positions Filter Wheel

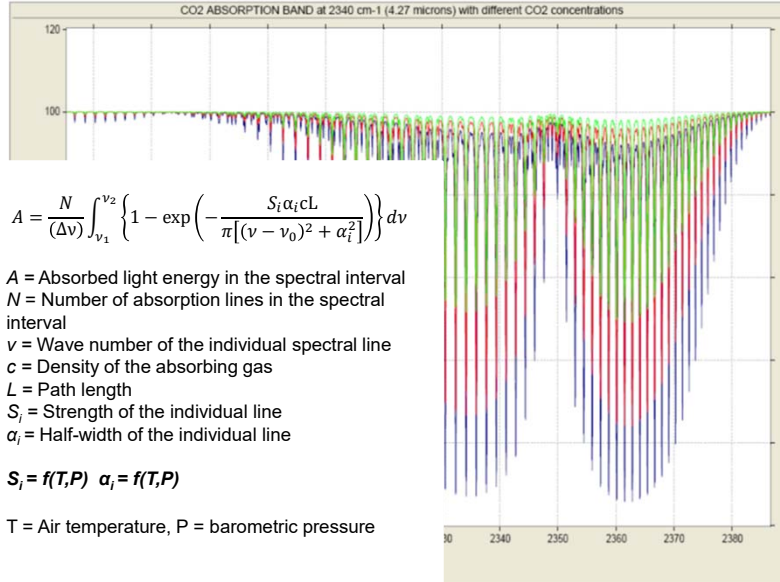


CO₂ active (absorbing)
 CO₂ reference (non-absorbing)
 H₂O: active (absorbing)
 H₂O: reference (non-absorbing)

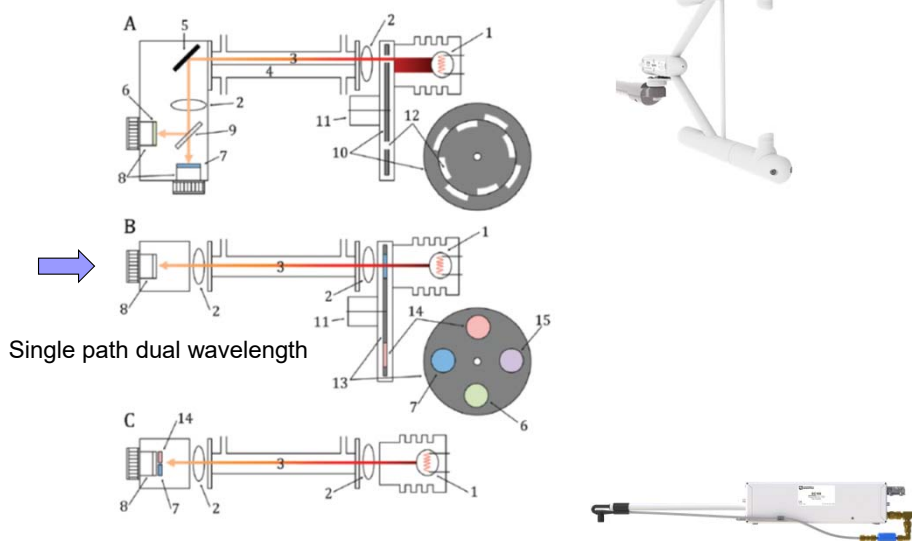
Gas Analyzer Measurement Principles



Gas Analyzer Measurement Principles



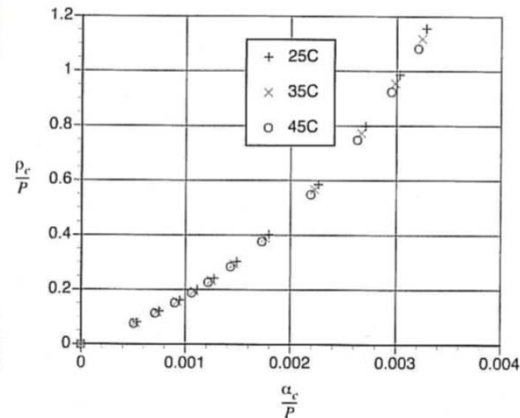
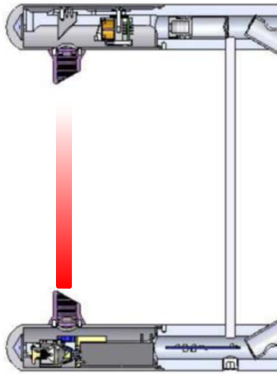
IRGA optical design schemes



Gas Analyzer Measurement Principles

$$\frac{\alpha_c}{P\psi} = h \left(\frac{\rho_c L}{P\psi} \right)$$

Infrared spectroscopy measures density in mol m^{-3} , not the required mixing ratios



Eddy Covariance Measurement Principles

Need to convert from density to mixing ratio. Instantaneous pressure and temperature of the mixture in the sensing path are required, but are not available for traditional open-path sensors.

$$e = \frac{\rho_v RT}{M_v} \quad \chi_c = \frac{\rho_c RT}{(P-e)M_c}$$

Point-by-point conversion of high frequency time series

$$F_c^{MR} = \frac{(P-e) \cdot m_c}{R \cdot \bar{T}} \cdot \overline{w' \chi_c'}$$

Closed-path analyzers
IRGASON due to the co-location of the sonic

$$F_c^{WPL} = \overline{w' \rho_c'} + \left(\frac{m_d \overline{\rho_c}}{m_v \overline{\rho_d}} \right) \overline{w' \rho_v'} + \left(1 + \frac{m_d \overline{\rho_v}}{m_v \overline{\rho_d}} \right) \overline{\rho_c} \frac{\overline{w'T'}}{\bar{T}}$$

For open-path sensors density terms (WPL) on 30 min fluxes. Pressure is neglected

$$\overline{w'T'} = \overline{w'T_c'} - 0.51 \bar{T} \overline{w'\chi_v'}$$

Correction of sonic temperature for humidity effects

Eddy Covariance Measurement Principles

Closed-path sensors: the air-temperature fluctuations are attenuated in the intake tubing. Temperature and pressure are measured in the sample cell

$$e = \frac{\rho_v RT}{M_v} \quad \chi_c = \frac{\rho_c RT}{(P-e)M_c}$$

Point-by-point conversion of high frequency CO₂ density time series

$$F_c^{MR} = \frac{(P-e) \cdot m_c}{R \cdot \bar{T}} \cdot \overline{w' \chi_c'}$$

All variables must be measured simultaneously

Must consider time lag and high-frequency attenuation in the intake tubing

This approach can be used with the IRGASON due to the co-location of the sonic

Eddy Covariance Measurement Principles

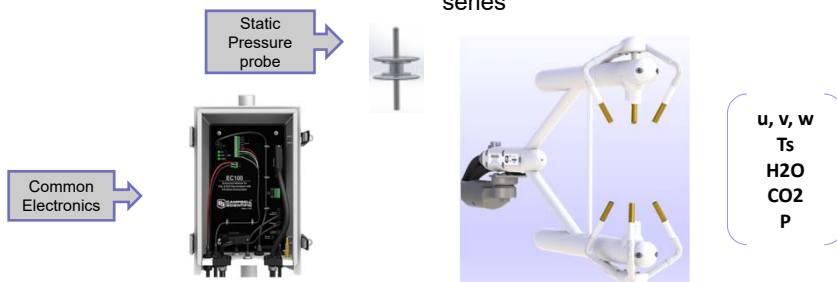
Open-path sensors with co-located sonic anemometer: the air-temperature fluctuations in the sample volume can be measured correctly

$$e = \frac{\rho_v RT}{M_v} \quad \chi_c = \frac{\rho_c RT}{(P-e)M_c}$$

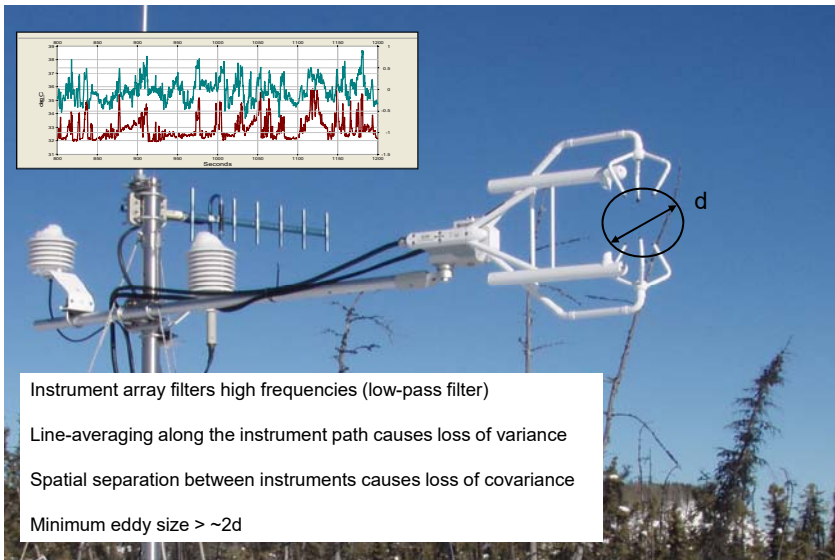
$$T_{av} = T \cdot \left(1 + \left(\frac{\gamma_v}{\gamma_d} - \frac{M_v}{M_d} \right) \cdot \frac{e}{p - \left(1 - \frac{M_v}{M_d} \right) \cdot e} \right)$$

$$F_c^{MR} = \frac{(P-e) \cdot m_c}{R \cdot \bar{T}} \cdot \overline{w' \chi_c'}$$

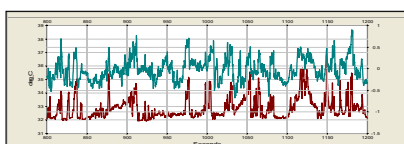
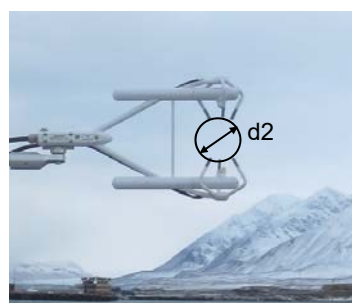
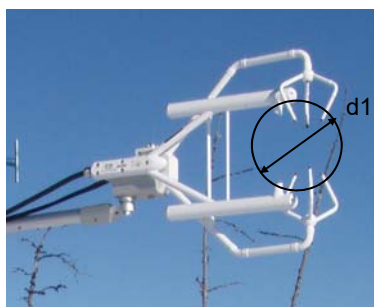
Point-by-point conversion of high frequency CO₂ density time series



Eddy Covariance Measurement Principles



Eddy Covariance Measurement Principles



Eddy Covariance Measurement Principles

Open-path sensors: subjected to the air-temperature fluctuations of the atmosphere. Fast-response air temperature is required: sonic BUT at a distance d

Separated by distance d
Low-pass filtered
Need spectral correction

In the same
sampling volume
and well
synchronized

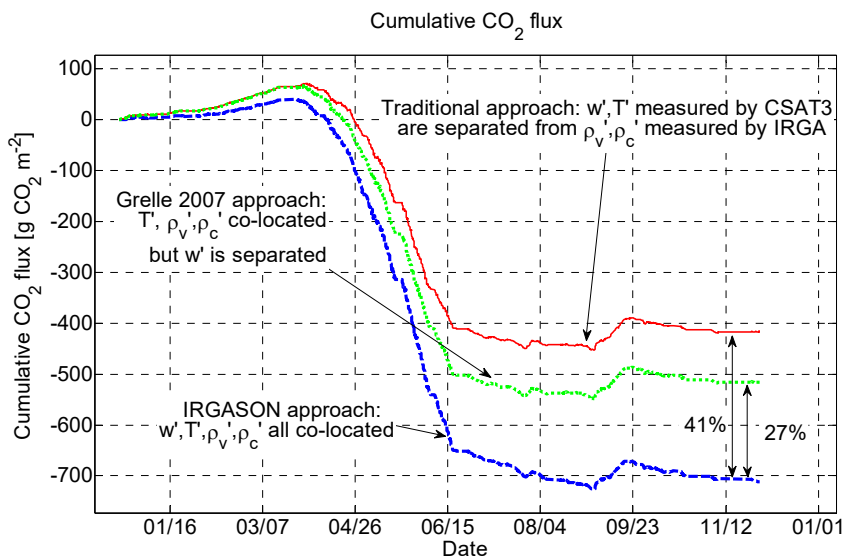
$$F_c^{WPL} = \overline{w' \rho_c'} + \left(\frac{m_d \overline{\rho_c}}{m_v \overline{\rho_d}} \right) \overline{w' \rho_v'} + \left(1 + \frac{m_d \overline{\rho_v}}{m_v \overline{\rho_d}} \right) \overline{\rho_c} \frac{\overline{w'T'}}{\overline{T}}$$

$$\overline{w'T'} = \overline{w'T_c'} - 0.51 \overline{T} \overline{w'\chi'_v}$$

Eddy Covariance Sensor Separation: Case Study

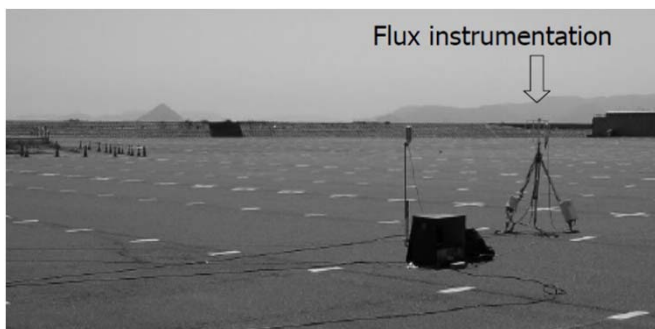


Eddy Covariance Sensor Separation



Eddy Covariance Experimental Verification

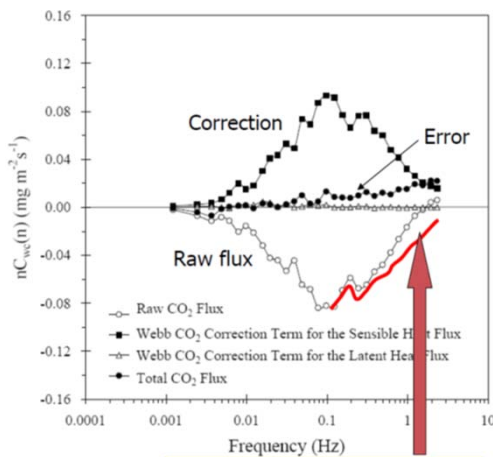
A case study- zero CO₂ flux over asphalt . Kondo & Tsukamoto (2008)



Eddy Covariance Experimental Verification

Measurements of heat, water vapor and CO₂ fluxes must have the same spectral and co-spectral response

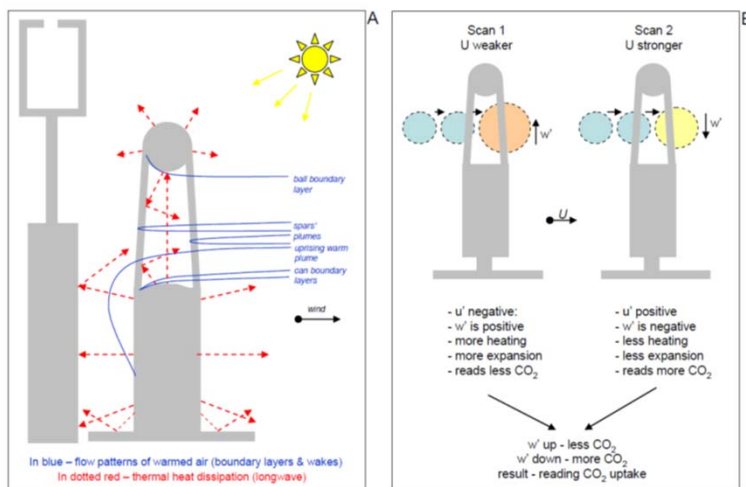
It is challenging when the corrections are large



Need to correct for loss of covariance before WPL correction

Eddy Covariance Instrumentation Biases

Example: Instrument surface heating causing apparent CO₂ uptake

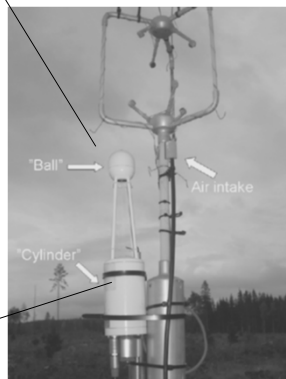


After Burba (2008)

Eddy Covariance Instrumentation Biases



Grelle and Burba (2007) installed a fine wire PRT in the sensing volume of the open-path analyzer to measure the extra heat generated by the lower cylinder



$$H_{PRT} = \rho c_p w' T'_{PRT} \text{ (W m}^{-2}\text{)}$$

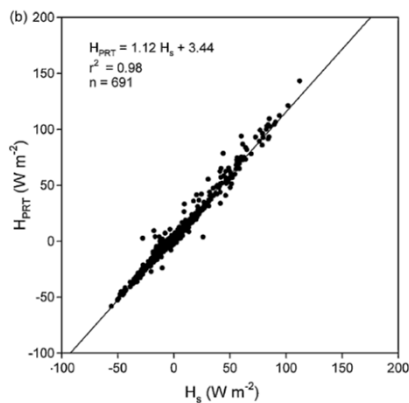
Eddy Covariance Instrumentation Biases



$$H_{PRT} = \rho c_p w' T'_{PRT} \text{ (W m}^{-2}\text{)}$$

$$F_{cnew} = F_{co} + 1.6077 \frac{E_{new}}{\rho_d} \frac{\rho_c}{1 + 1.6077(\rho_v/\rho_d)} + \frac{H_{PRT}}{\rho c_p} \frac{\rho_c}{T_a} \quad (1)$$

$$E_{new} = \left(1 + 1.6077 \frac{\rho_v}{\rho_d} \right) \left(E_o + \frac{H_{PRT}}{\rho c_p} \frac{\rho_v}{T_a} \right) \quad (2)$$



Grelle and Burba (2007)

Eddy Covariance Instrumentation Biases

Ma, J. et al. (2014). A downward CO₂ flux seems to have nowhere to go. *Biogeosciences*, 11: 6251-6262.

Chinese Scientists Discover Carbon Sequestration Hidden under the Desert

Jul 31, 2015

Email Print Text Size Share

According to Chinese Academy of Sciences, a study led by the Institute of Ecology and Geography has discovered the "Carbon Sequestration" stored in saline aquifers in the desert that the world's scientists have been struggling to search for decades. This finding creates a new direction on the research on "Carbon Sequestration".

Of the carbon dioxide produced by fossil fuel combustion, one part is stored to the atmosphere (causing atmospheric carbon dioxide concentrations to increase), one part goes to the ocean, but there are still some carbon dioxide disappeared. For decades, scientists have tried to find "the lost carbon sinks", and have basically reached the agreement that it's in terrestrial ecosystems.

Until a few years ago, Chinese and American scientists discovered that there's CO₂ flux entering into the surface of the desert region, inferring that a big carbon sink may exist in the desert. These findings bring also the question that how it is possible for sparse plants in the barren desert to absorb the carbon dioxide at such a large quantity.

After ten years' study, the research team led by Li Yan, researcher from Institute of Ecology and Geography of Chinese Academy of Sciences, has found the answer: the "Carbon Sequestration" is stored in saline aquifers in the desert.

"The total amount of the Carbon Sequestration in desert is estimated to be up to 100 billion tons worldwide, which becomes the third active carbon sinks besides plants and soil," said Li Yan. (People's Daily Online)

(Editor: 王)

Li Yan

Xinjiang Institute of Ecology and Geography
E-mail: liyan@ms.xj.ac.cn

Reference

Hidden carbon sink beneath desert

Related Articles



Humans Accidentally Created Hidden Carbon Sink in the Desert

Jul 30, 2015

"Basically, people thought the whole area and region is totally negligible to the global carbon budget," says Yan Li of the Chinese Academy of Sciences in Urumqi, China. "We are arguing that that's not the case." Li

Eddy Covariance Instrumentation Biases?

Ma, J. et al. (2014). A downward CO₂ flux seems to have nowhere to go. *Biogeosciences*, 11: 6251-6262. **The desert is a carbon sink**



$$F_{\text{cnew}} = F_{\text{co}} + 1.6077 \frac{E_{\text{new}}}{\rho_d} \frac{\rho_c}{1 + 1.6077(\rho_v/\rho_d)} + \frac{H_{\text{PRT}}}{\rho c_p} \frac{\rho_c}{T_a}$$

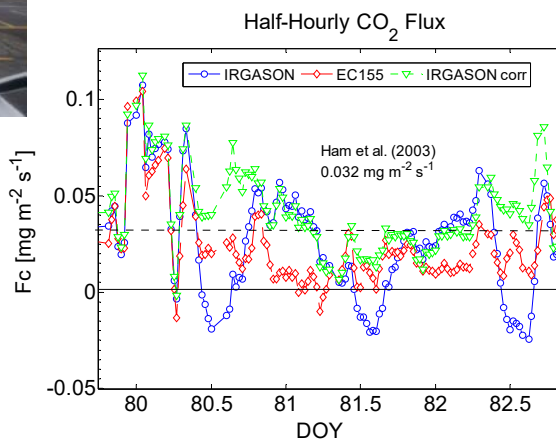
$$E_{\text{new}} = \left(1 + 1.6077 \frac{\rho_v}{\rho_d} \right) \left(E_o + \frac{H_{\text{PRT}}}{\rho c_p} \frac{\rho_v}{T_a} \right)$$

Schlesinger, W. (2016). An evaluation of abiotic carbon sinks in deserts. *Global Change Biol.*, doi: 10.1111/gcb.13336 **We can't find the carbon?**

Eddy Covariance Instrumentation Biases

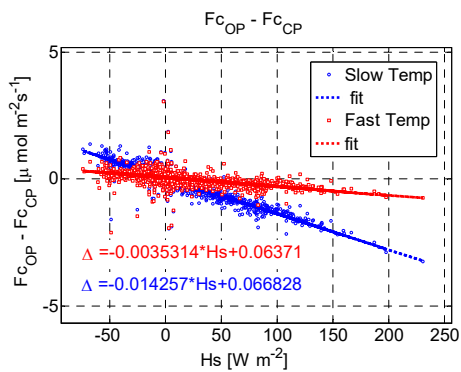
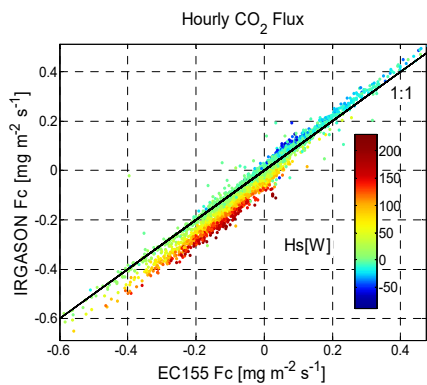


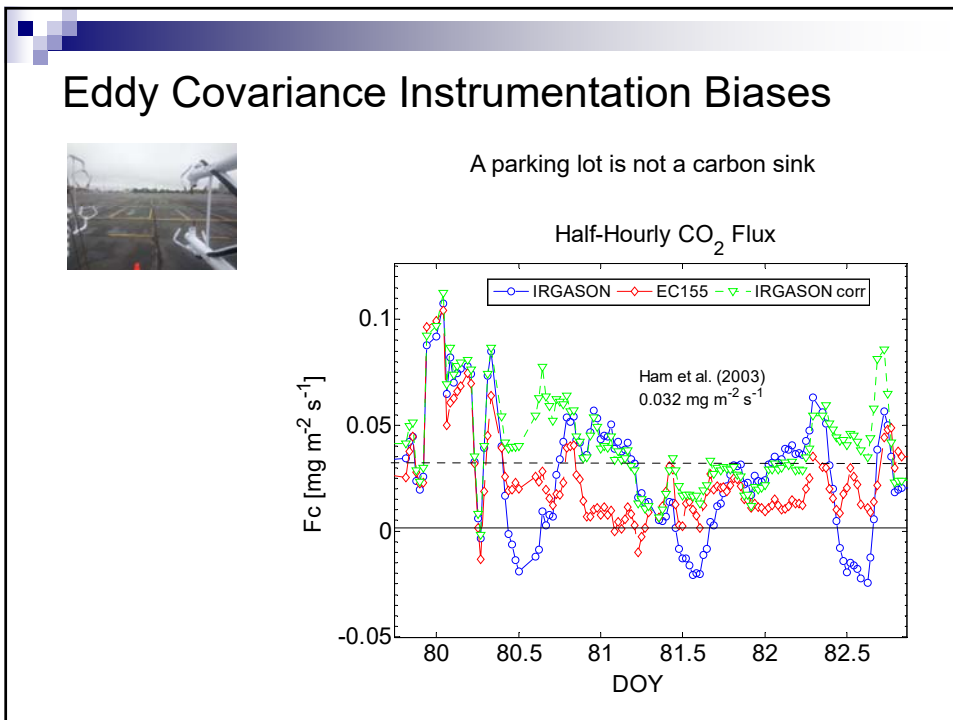
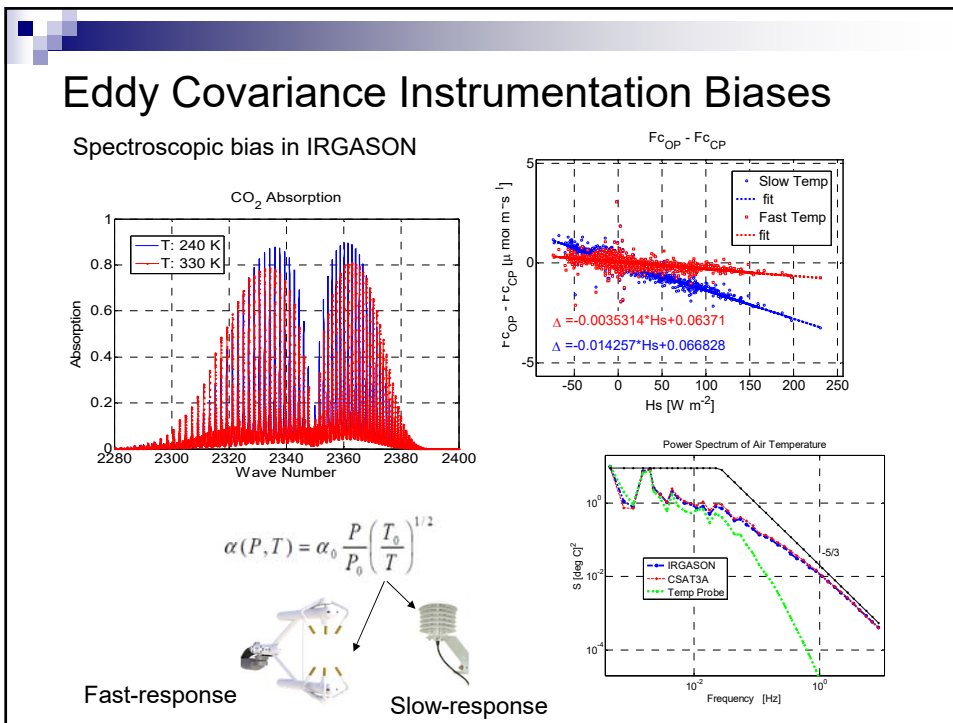
A parking lot experiment: Where is the carbon?



Eddy Covariance Instrumentation Biases

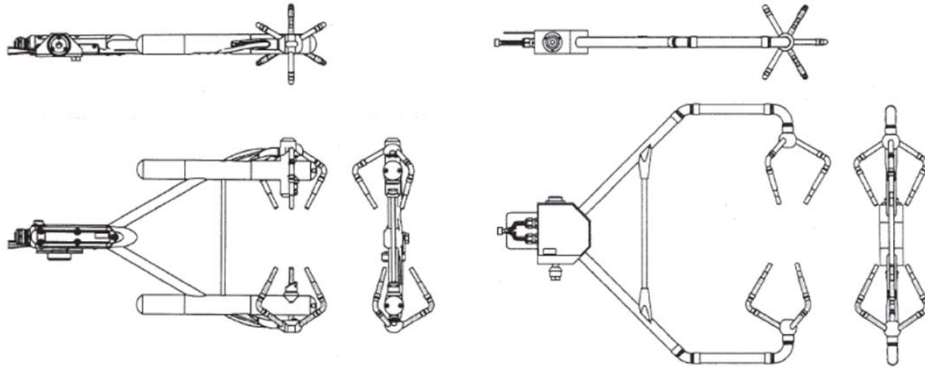
Open-path and closed-path comparison





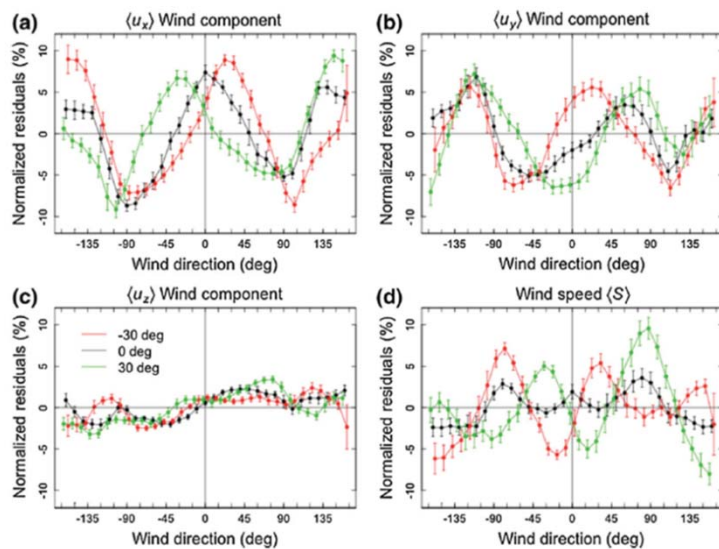
Eddy Covariance Instrumentation Biases

Example: Flow distortion causing artificial cross correlations between u' and v'

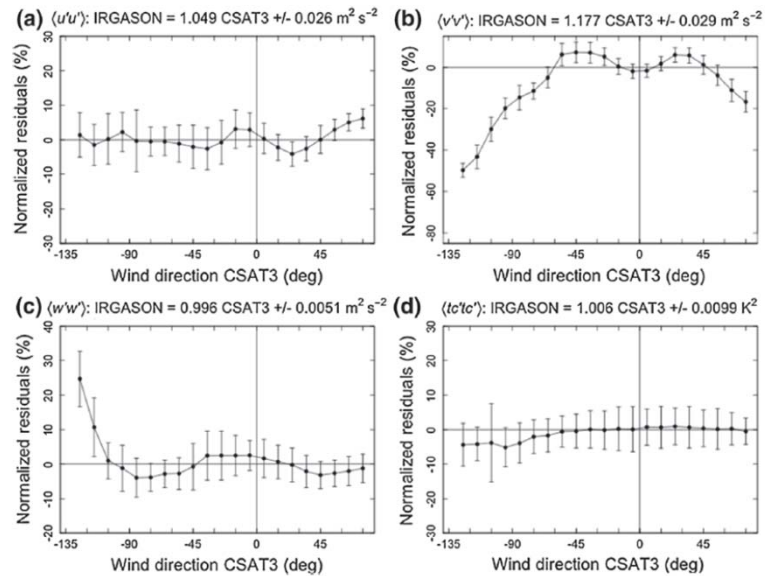


Eddy Covariance Instrumentation Biases

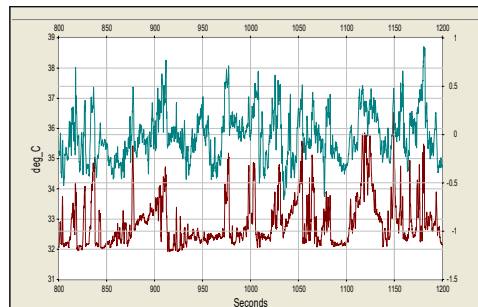
Example: Flow distortion errors



Eddy Covariance Instrumentation Biases



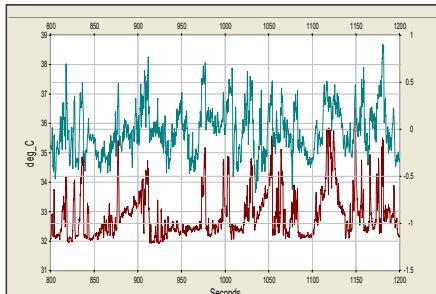
Instrument Requirements



Perfect instruments should:

- Be invisible (or very small) so that it does not affect the flow (create or destroy eddies) and not average small eddies in the sensing path
- Be fast-response to capture the rapid changes in the measured quantities
- Be sensitive to small changes in measured quantities
- Be highly accurate, stable, linear and unaffected by environmental factors (temperature, precipitation, dust, etc.)

Instrument Requirements



Perfect instruments should:

- Make all measurements simultaneously and in the same point in space (preserve covariance)
- Consume no power
- Operate forever with no maintenance or calibration under all conditions
- Easy to operate

Instrument Selection Guide and Tradeoffs



'Know Thy Site' 'Know Thy Sensor'



Ray Leuning

Most Flux Instruments are Very Good;
Pick the Instrument System that is Most Appropriate to Your Weather and Climate

And thy methods, tools, model assumptions and experiments!

Some instruments are better than others. Pick the instrument that is right for You.

Consider:

- Site conditions (rain, Hs, CO₂ flux, canopy...)
- Power budget
- Scientific objectives (uncertainties)
- Cost of operation, maintenance, calibration

Open- or Closed-Path System?



Open-path Systems

Sonic and gas analyzer separate



Or co-located



Open-path systems

Advantages:

- Excellent spectral response
- Low power consumption
- Less complex (no pumps, tubing and filters)
- Lower cost
- Low maintenance
- No tube delays and minimal time lag (scales with wind)



Disadvantages:

- Data loss due to precipitation, dust, birds, insects (data spikes and drift)
- Larger density corrections
- No possibility for automated field calibrations

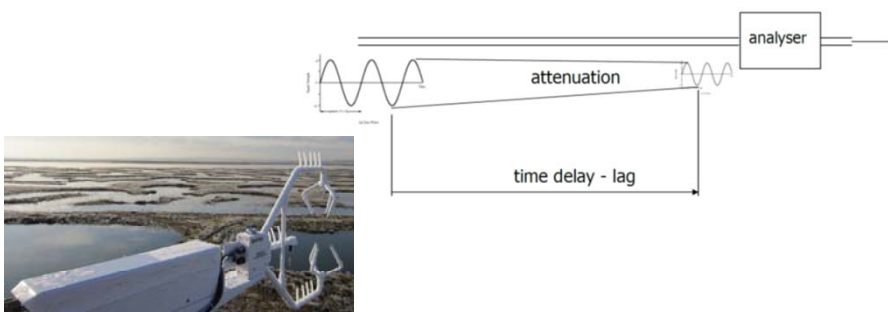
Closed-path Systems with Short Intake Tube



Advantages:

- Not affected by precipitation, dust, birds (less data spikes) But the sonic might be!
- Temperature fluctuations are attenuated in the intake tube - smaller density corrections
- Calculate mixing ratio in real time
- Possibility for automated field calibrations

Closed-path Systems with Short Intake Tube



High-frequency attenuation and time lag depend on flow rate, tube diameter and length, tube material, RH (becomes worse as dirt accumulates on the filter!)

Different attenuation and lags for CO_2 and H_2O especially in at high RH regimes

Closed-path Systems with Short Intake Tube



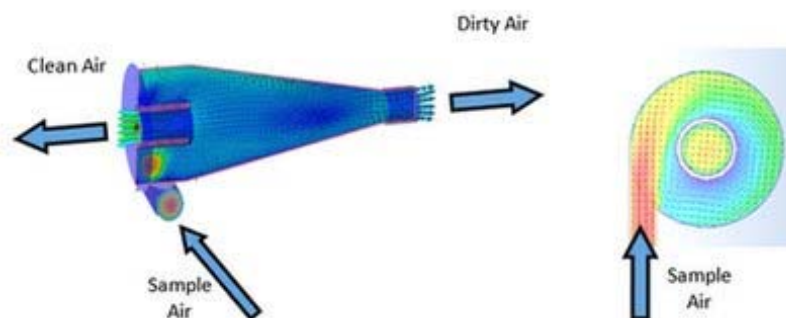
Disadvantages:

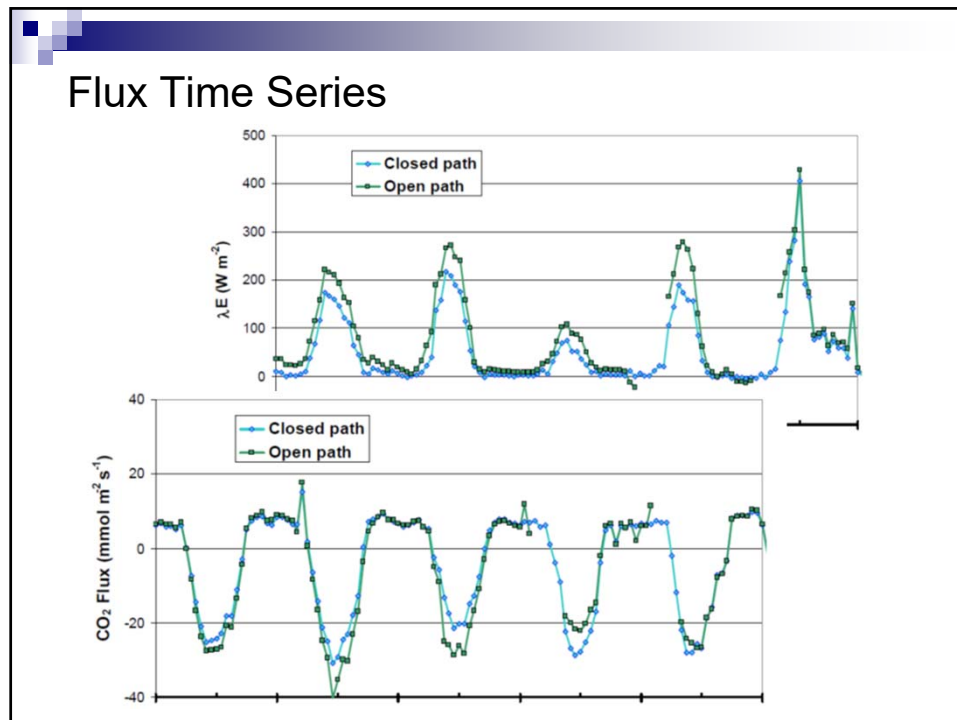
- Loss of frequency response due to tube attenuation and accumulation of particulates on the face of the filter (worse for water)
- Changing lag due to changes in flow
- Higher power requirements due to the pump
- Loss of synchronicity due to time variable lags
- Higher cost and increased maintenance (filters, pump, tubing)

Closed-path Gas Analyzer Vortex Intake



Particle separation based on size and mass
No accumulation of particulate matter
Constant flow conditions





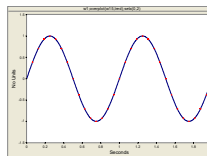
Math Tools and Concepts

- **Variance and Covariance**
- **Spectral Decomposition:** changing from time to frequency domain to identify instrumentation issues
- **Aliasing errors due to discrete sampling:** signals not measured at the correct frequency

Calculate Variation of a Signal or a Co-Variation Between Two Signals

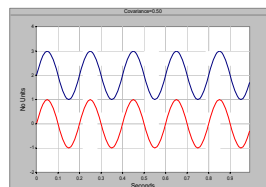
- **Variance:** A measure of how a signal varies about its mean

$$\text{Var}(x) = \frac{1}{N} \sum_{k=1}^N [x(k) - \bar{x}]^2$$

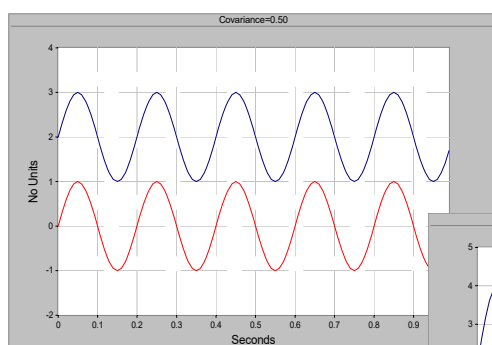


- **Covariance:** A measure of how two signals vary together about their means

$$\text{CoVar}(x, y) = \frac{1}{N} \sum_{k=1}^N [x(k) - \bar{x}][y(k) - \bar{y}]$$

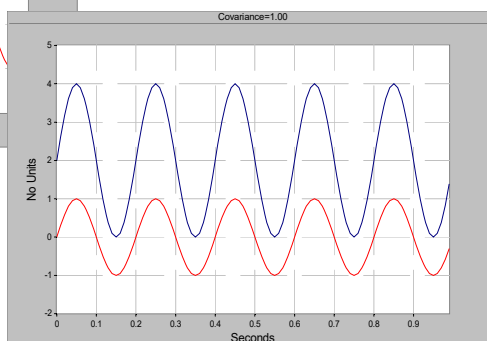


Covariance - Amplitude Attenuation

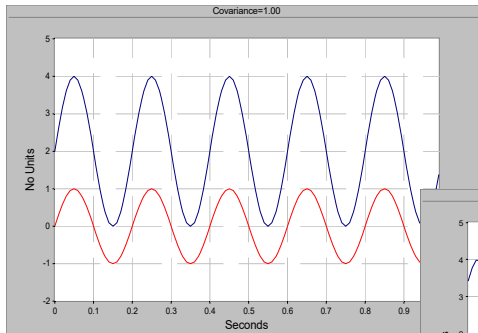


Covariance = 0.50

Double the variation of
one signal
Covariance = 1.00

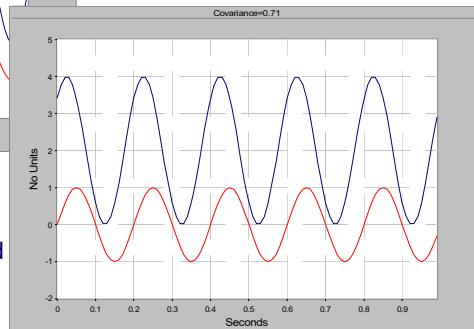


Covariance - Signal Time Delay

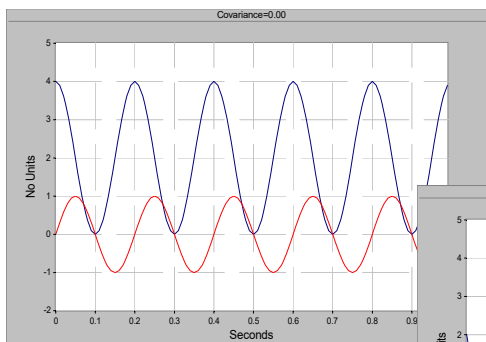


Two signals perfectly synchronized
Covariance = 1.00

Time shift one signal by 1/8 of the period
Covariance = 0.71

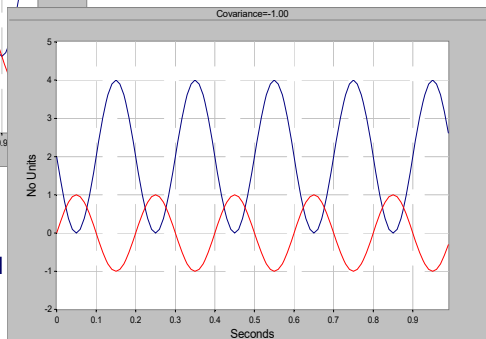


Covariance - Signal Time Delay



Time delay by 1/4 of a period
Covariance = 0.00

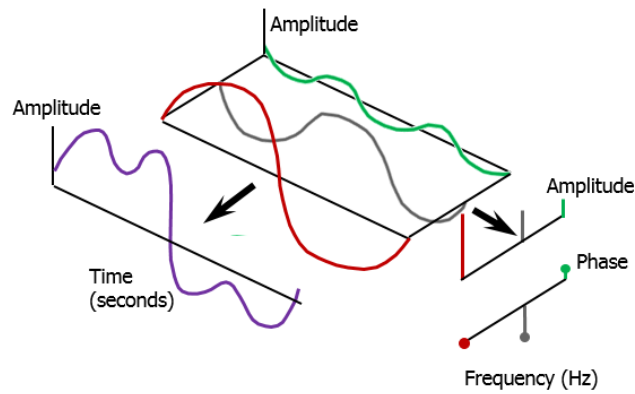
Time shift one signal by 1/2 of a period
Covariance = -1



Spatial separation is equivalent to a time delay

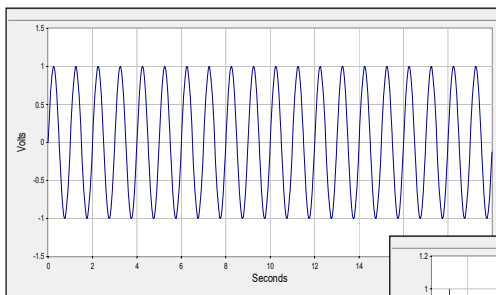
Spectral Decomposition of a Time Series

Fourier Transform



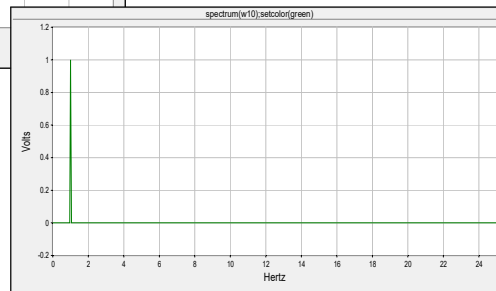
$$s_a(t) = k_a + A_{a_1} \cos(\omega_{a_1} t + \phi_{a_1}) + A_{a_2} \cos(\omega_{a_2} t + \phi_{a_2}) + A_{a_3} \cos(\omega_{a_3} t + \phi_{a_3}) + \dots$$

Spectral Decomposition of a Sine Wave

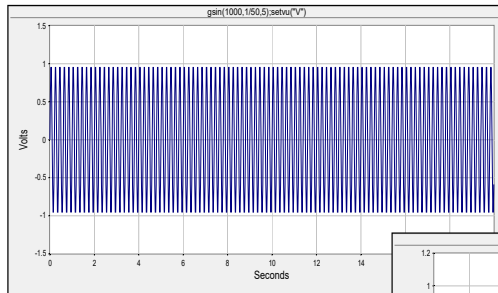


1-Hz Sine Wave as a function of time

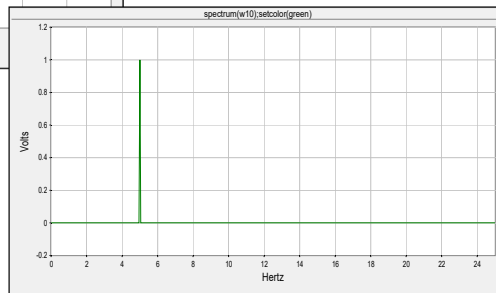
1-Hz Sine Wave as a function of frequency



Spectral Decomposition of a Sine Wave

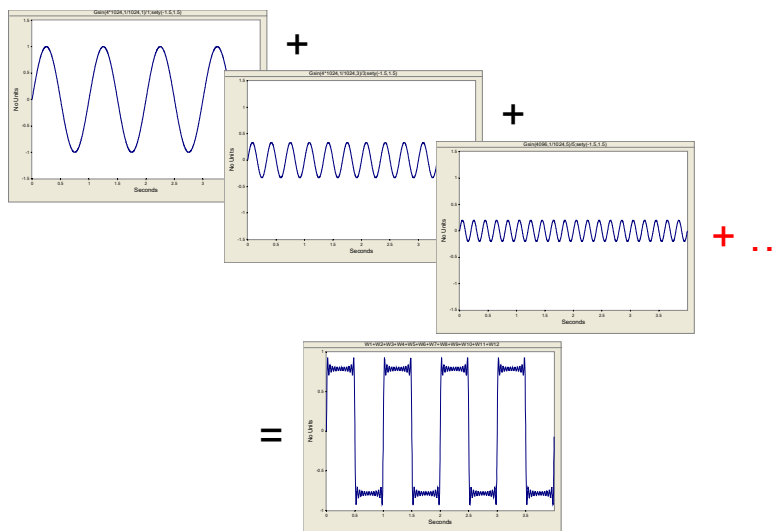


5-Hz Sine Wave as a function of time

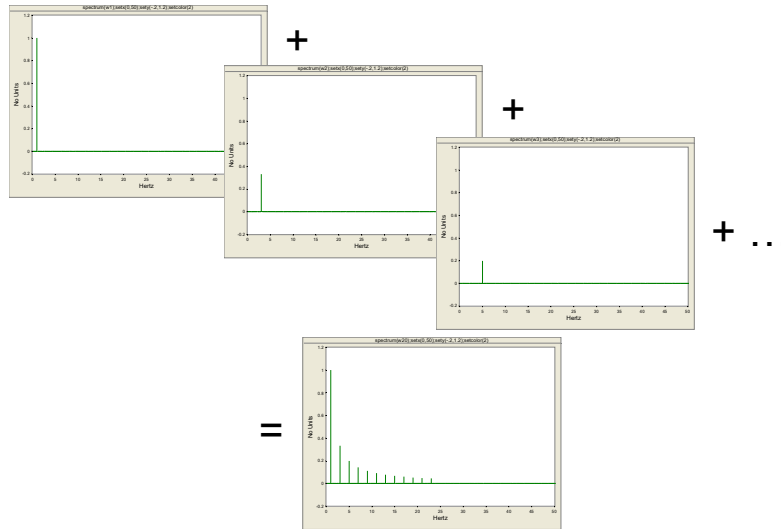


5-Hz Sine Wave as a function of frequency

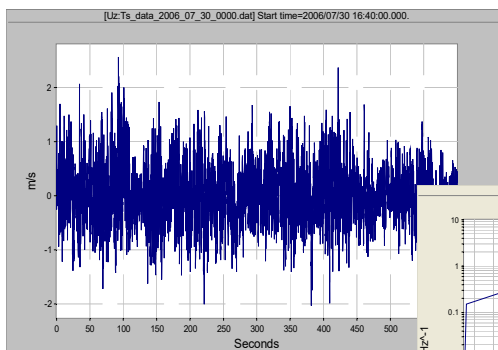
Spectral Decomposition of a Periodic Signal



Spectral Decomposition of a Periodic Signal

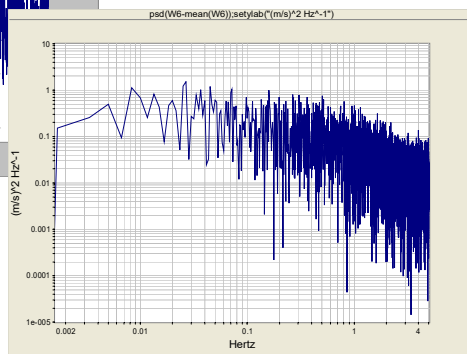


Vertical Wind

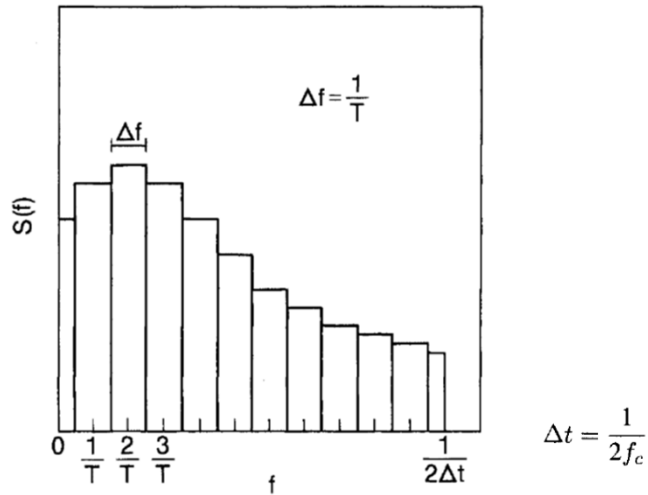


As a function of time

As a function of frequency
(phase not shown)

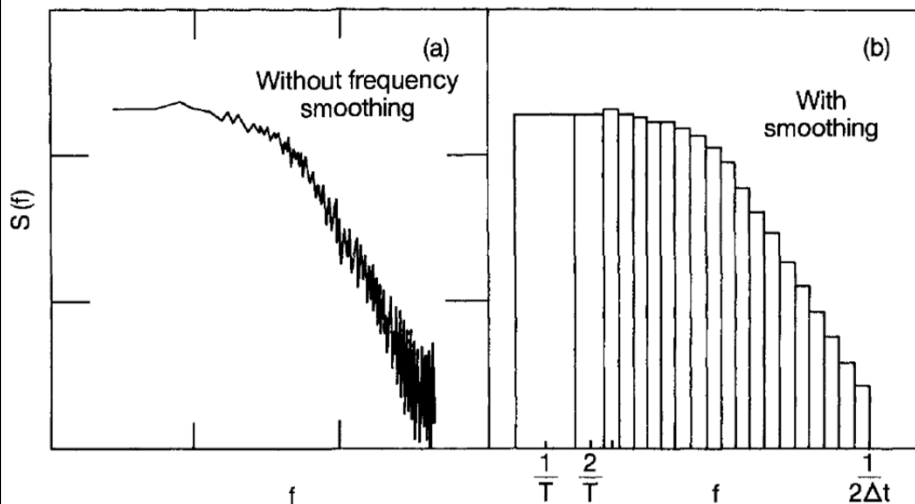


Spectral Resolution



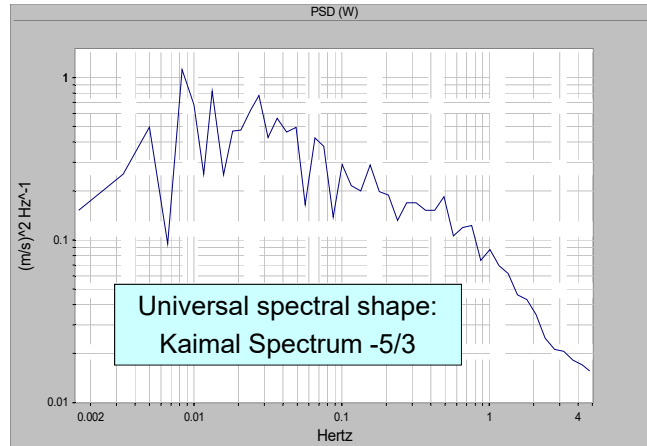
Length of the time series T determines the spectral resolution Δf and the sampling period Δt determines the maximum frequency

Spectral Smoothing of a "Raw" Spectrum



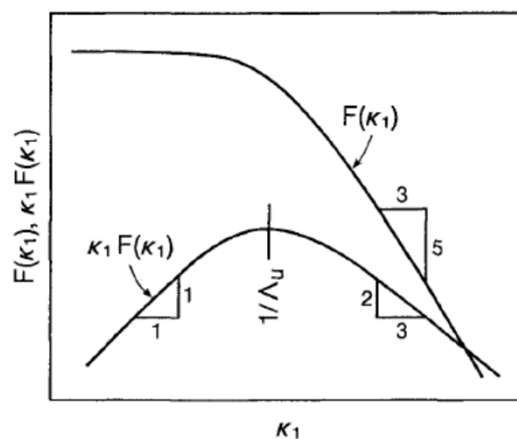
Scatter is reduced by averaging a frequency window that expands in width with frequency (log scales)

Spectral Smoothing of a "Raw" w Spectrum



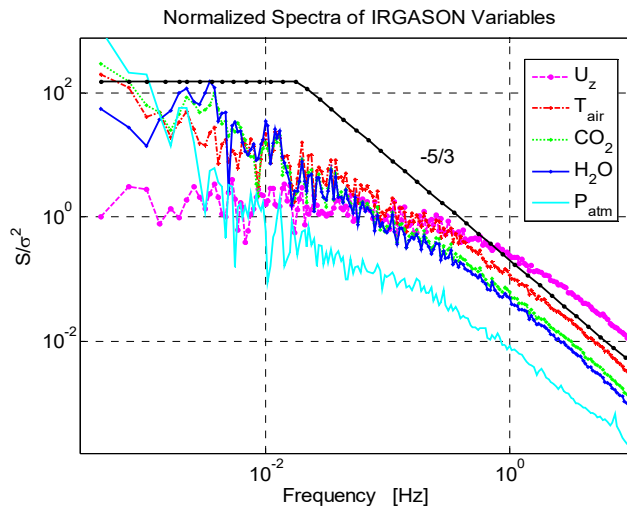
$S(f)$ Spectral density $A^2/\Delta f$ (units of variance per Δf)
 Area under the curve = variance
 Sometimes frequency weighted spectrum is used $fS(f)$ (units of variance)

Frequency Weighted Spectrum

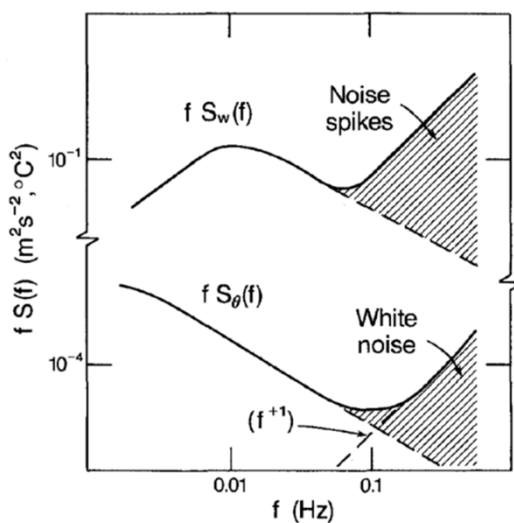


Frequency weighted spectrum is shows the spectral gap at the low frequency range

Spectral Similarity



High-frequency Distortion due to Instrumental Effects



Noise spikes in sonic w measurement (bug or precipitation)

Noise floor of PRT temperature measurement

Spectral Decomposition - Co-spectra

- We can compute covariance in the time domain or the frequency domain.

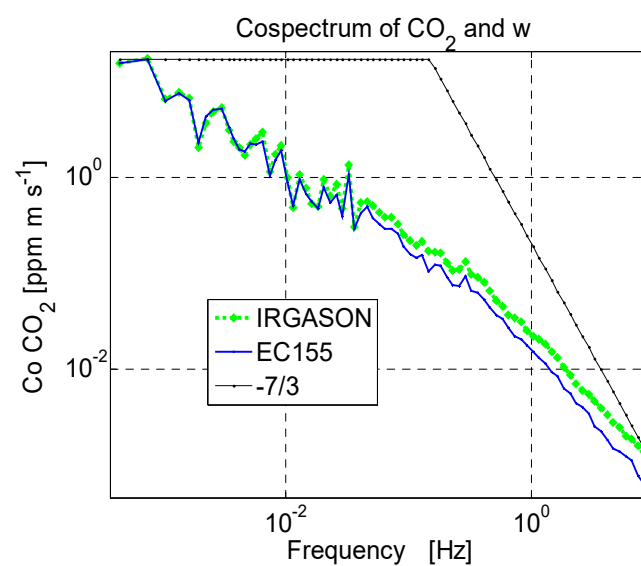
$$s_a(t) = k_a + A_{a_1} \cos(\omega_{a_1} t + \phi_{a_1}) + A_{a_2} \cos(\omega_{a_2} t + \phi_{a_2}) + A_{a_3} \cos(\omega_{a_3} t + \phi_{a_3}) + \dots$$

$$s_b(t) = k_b + A_{b_1} \cos(\omega_{b_1} t + \phi_{b_1}) + A_{b_2} \cos(\omega_{b_2} t + \phi_{b_2}) + A_{b_3} \cos(\omega_{b_3} t + \phi_{b_3}) + \dots$$

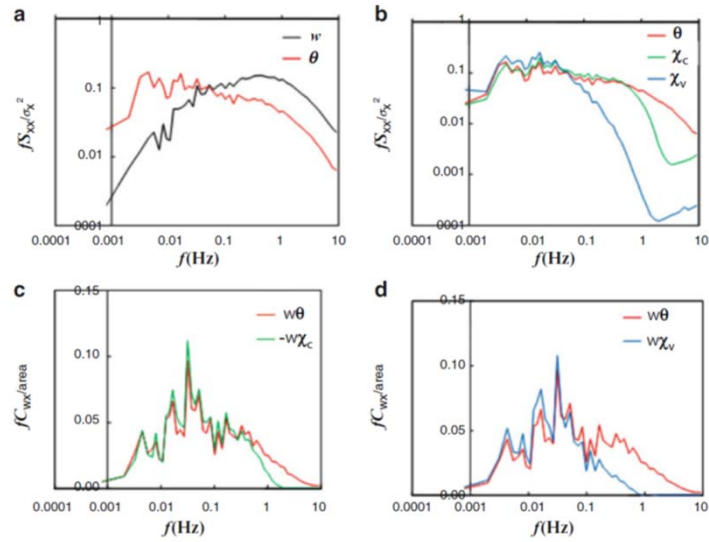
$$\text{cov}(s_a, s_b) = \left[\frac{A_{a_1} A_{b_1}}{2} \cos(\phi_{a_1} - \phi_{b_1}) \right]_{\omega_{a_1} = \omega_{b_1}} + \left[\frac{A_{a_2} A_{b_2}}{2} \cos(\phi_{a_2} - \phi_{b_2}) \right]_{\omega_{a_2} = \omega_{b_2}} + \left[\frac{A_{a_3} A_{b_3}}{2} \cos(\phi_{a_3} - \phi_{b_3}) \right]_{\omega_{a_3} = \omega_{b_3}} + \dots$$

- The covariance computed in the time domain equals the area under the curve of a Co-Power Spectral Density function (CoPSD).

Co-Spectral Analysis



Frequency Weighted Co-Spectra

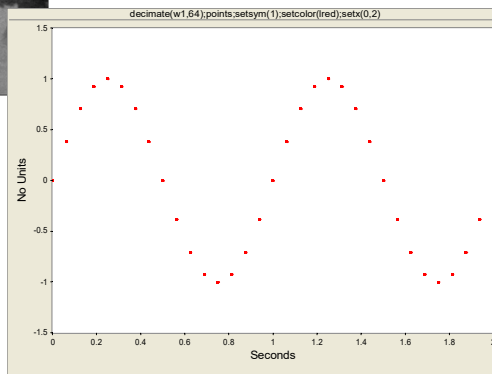


After Leuning

Aliasing – Discrete Time-Sampled Signal



What is the shape of the measured signal ?



Aliasing – Discrete Time-Sampled Signal

w1.overplot(w15,red);setx(0.2)

decimate(w1,64);points;setym(1);setcolor(red);setx(0.2)

What is the true shape of the original signal?

Aliasing – Discrete Time-Sampled Signal

-Gain(4*1024,1/1024,15)/1;sety(-1.5,1.5);overplot(w15,red);setx(0.2)

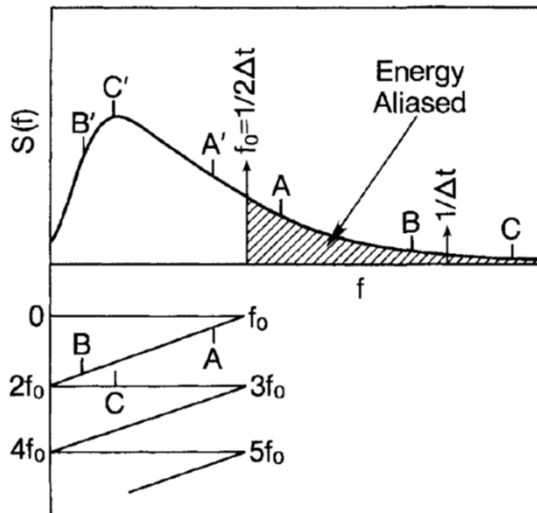
decimate(w1,64);points;setym(1);setcolor(red);setx(0.2)

What is the true shape of the original signal?

Folding of Spectral Energy

Misrepresentation of the high frequency components

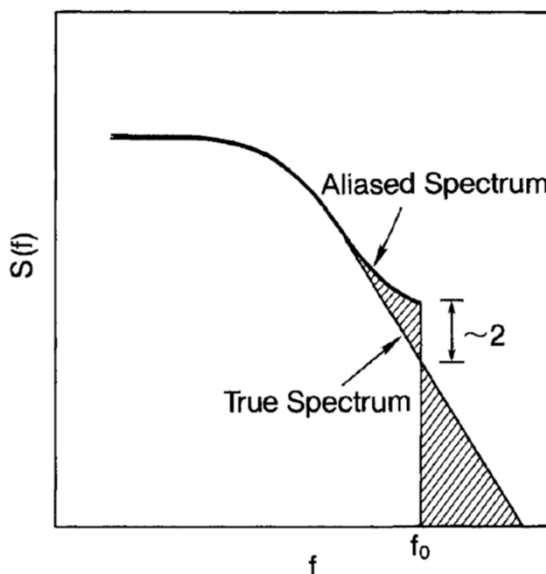
f_0 – Nyquist frequency
 $f_0 = f_{\text{sample}}/2$
 For proper frequency representation
 $f_{\text{sample}} = 2f_{\text{max}}$



Folding of Spectral Energy

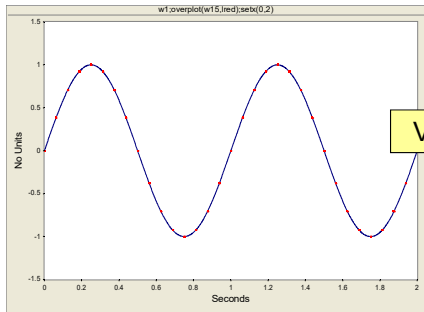
Misrepresentation of the high frequency components

The variation of the signal is preserved, so aliasing is not a problem for calculating fluxes

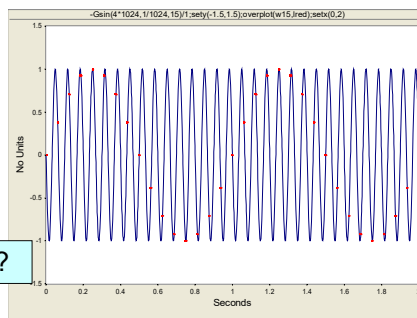


Folding of Spectral Energy

Misrepresentation of the rate at which the signals are changing

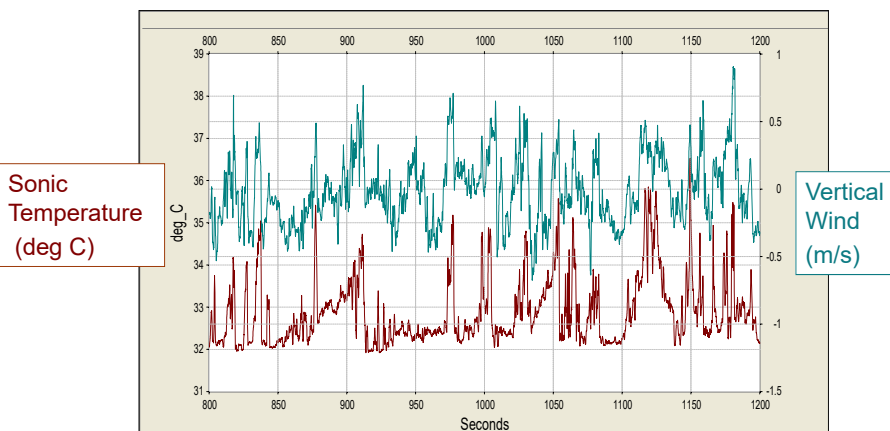


Variances and covariances are correct



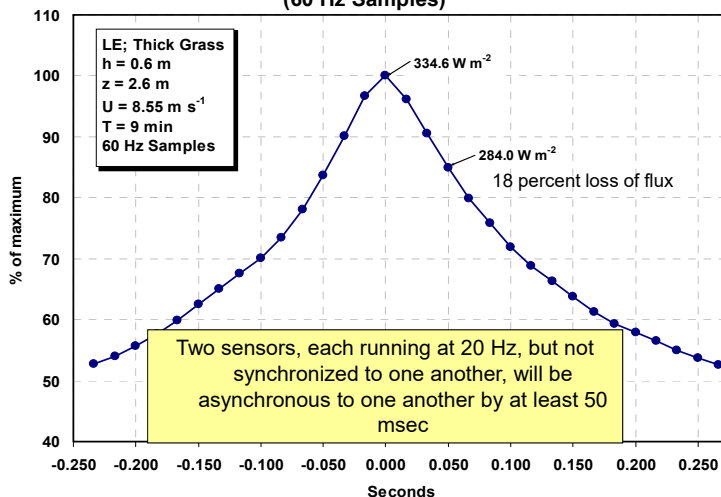
Eddy Covariance System Requirements

Adequate frequency response of the sensors (small d, high flow)
 Preserve temporal and spatial correlation of vertical wind and scalar



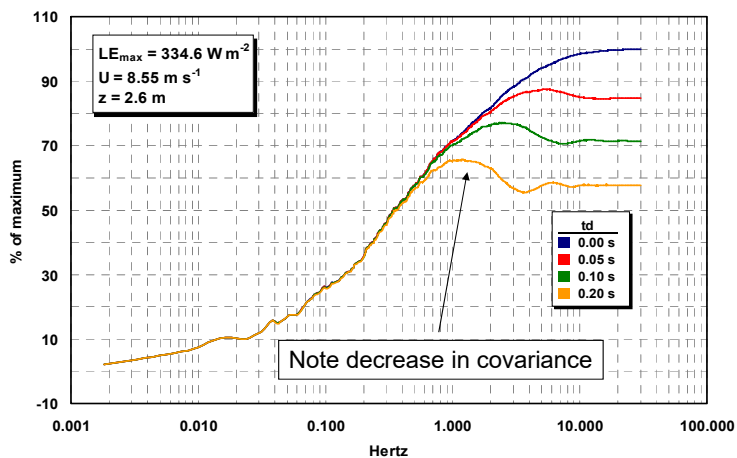
Eddy Covariance System Requirements

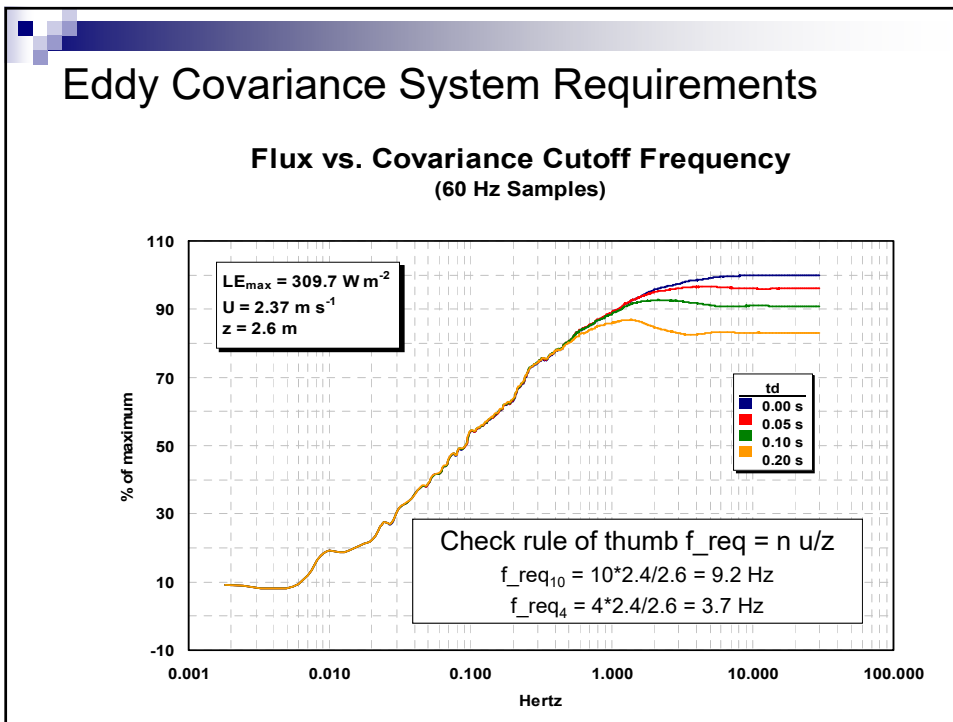
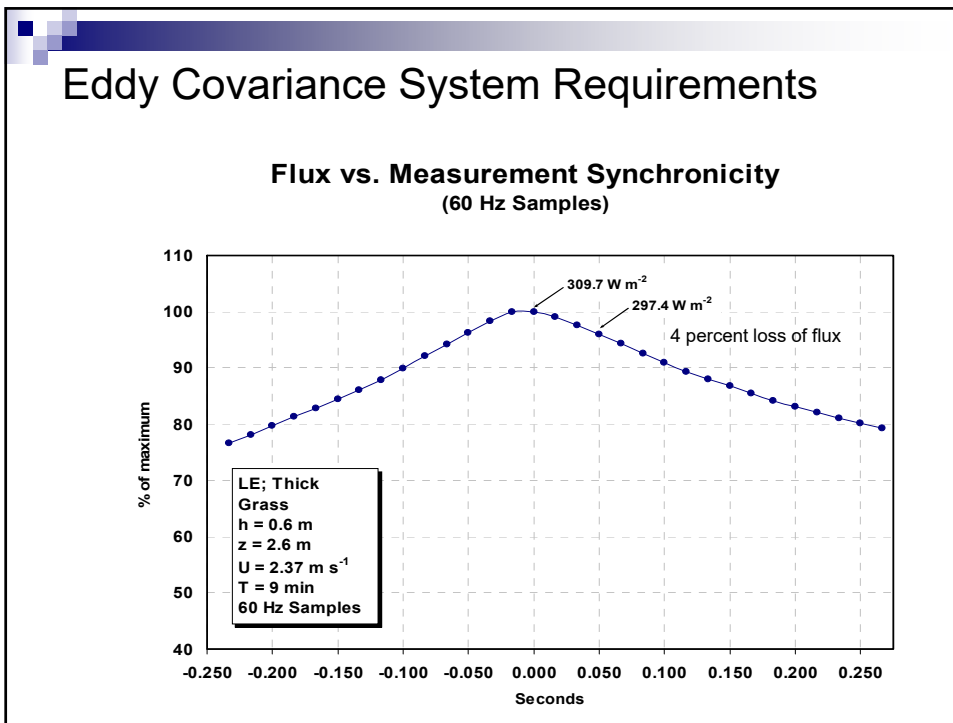
Flux vs. Measurement Synchronicity
(60 Hz Samples)



Eddy Covariance System Requirements

Flux vs. Covariance Cutoff Frequency
(60 Hz Samples)





Summary

- Know the limitations and the assumptions of the method
- Know thy site (heterogeneity, advection, storage)
- Select instruments appropriate for your conditions and research goals (adequate frequency response, temporal and spatial synchronization)
- Know your instruments (test in lab conditions, intercompare, calibrate and maintain)
- QC your data (spectra, co-spectra, stationarity, advection, instrument effects)

Outlook after T. Foken:

The knowledge of the fathers of the eddy-covariance method is often forgotten and errors of the first days of the method are repeated

Four Problems of the Eddy-covariance Technique

- Energy balance closure (not always an instrument problem)
- Night-time fluxes (sweeps systematic bias)
- Heterogeneous terrain (larger scales and secondary circulations)
- Accuracy of the method

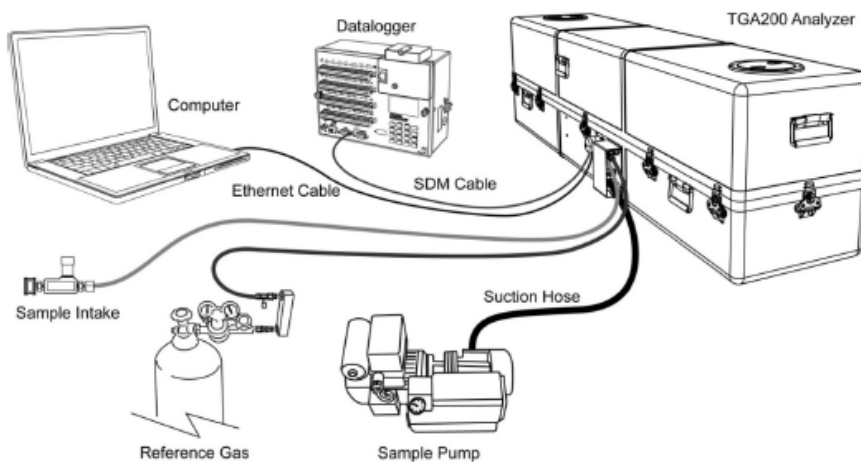
Trace Gas Analyzer (TGA) for CH₄, N₂O and 13C Isotope Measurements



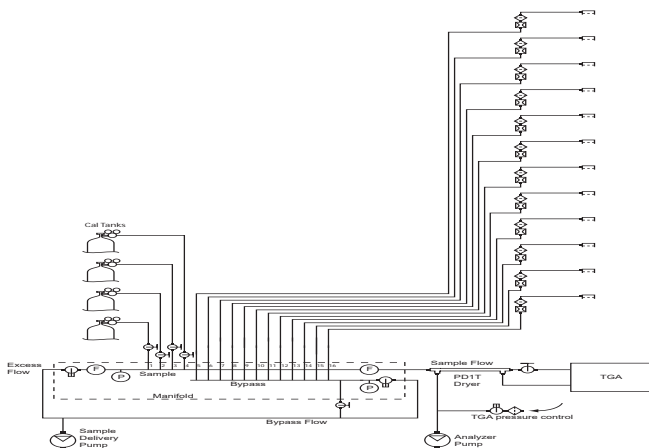
What is a TGA?

CSI has been manufacturing TGA's since 1993
 TGA is a tunable diode laser absorption spectrometer (TDLAS), and new lasers are TE cooled
 They are rugged, portable, and designed for use in the lab or out in the field
 Uses a small sample cell volume for good frequency response no mater the application

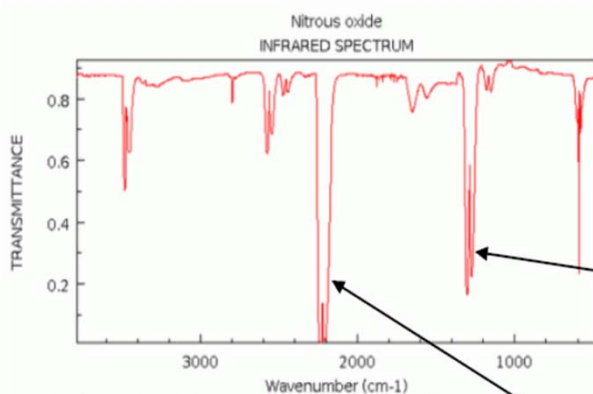
System Components for CH₄, N₂O and 13C Isotope Measurements



System Components for CH₄, N₂O and ¹³C Isotope Measurements from Multiple Inputs



Infrared Spectrum of CH₄, N₂O



NIST Chemistry WebBook (<http://webbook.nist.gov/chemistry>)
N₂O Spectrum in the mid-IR range.

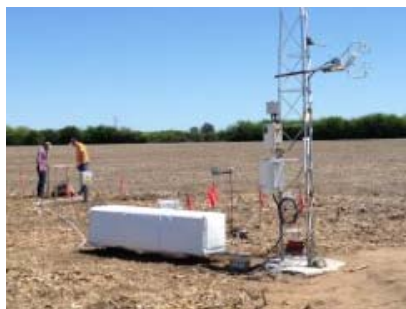
Absorption band used for N₂O/CH₄ measurements.

Stronger absorption band used for N₂O-only measurements.

Example Configurations & Applications

- Argentina (N₂O/CO₂, Eddy Covariance)
- Australia (CO₂ Isotopes, Leaf Chamber)
- Minnesota (Methane, Eddy Covariance)
- Brazil (N₂O/CO₂, Multi-Site Gradient)
- Example Pump Shelters

Example Configurations & Applications



LOCATION: NORTHEAST ARGENTINA

RESEARCH: UNDERSTAND NITROGEN AND CARBON CYCLES FOR CORN AND SOYBEAN ROTATIONS AND VARIOUS TILLAGE/FERTILIZER PRACTICES

MAJOR SYSTEM COMPONENTS: TGA200 ANALYZER, CSAT3 3D SONIC ANEMOMETER, FW05 FINEWIRE THERMOCOUPLE, LI-7500A, TIPPING RAIN BUCKET, NET RADIOMETER, SOIL MOISTURE PROBES, SOIL HEAT FLUX PLATES, SOIL TEMPERATURE PROBES

Example Configurations & Applications



LOCATION: NORTHEAST ARGENTINA
RESEARCH: UNDERSTAND NITROGEN AND CARBON CYCLES FOR CORN AND SOYBEAN ROTATIONS AND VARIOUS TILLAGE/FERTILIZER PRACTICES
MAJOR SYSTEM COMPONENTS: TGA200 ANALYZER, CSAT3 3D SONIC ANEMOMETER, FW05 FINEWIRE THERMOCOUPLE, TIPPING RAIN BUCKET, NET RADIOMETER, SOIL MOISTURE PROBES, SOIL HEAT FLUX PLATES, SOIL TEMPERATURE PROBES